A Thesis

on

An Experimental Study on Effects of Thermal Cycling on Cast Aluminium Composites Reinforced with Silicon Carbide and Fly Ash Particles

Submitted in partial fulfilment of the requirement for the award of the Degree of

MASTER OF ENGINEERING
IN
PRODUCTION AND INDUSTRIAL ENGINEERING

Submitted By
Sanjeev Kumar
Univ. Reg No. 800882013

Under Guidance of

Sh.Bikramjit Sharma
Assistant Professor
Thapar University, Patiala

DEPARTMENT OF MECHANICAL ENGINEERING
THAPAR UNIVERSITY
PATIALA-147004, INDIA

CERTIFICATE

This is to certify that the work in this Thesis report entitled "An Experimental Study on Effects of Thermal Cycling on Cast Aluminium Composites Reinforced With Silicon Carbide and Fly Ash Particles " submitted in partial fulfilment of requirement for the award of **Master of Engineering in Production and Industrial Engineering** in the Mechanical Engineering Department at Thapar University, Patiala, is an authentic record of work carried out by me under the guidance of **Sh. Bikramjit Sharma, Asstt.Professor, Mechanical Engineering Department, Thapar University, Patiala.**

The matter embodied in this report has not been submitted in part or full to any other university or institute for the award of any degree.

Sanjeev Kumar

Dated: 15/07/2010 **(Sanjeev Kumar)**

This is to certify that above declaration made by the student concerned is correct to the best of my knowledge & belief.

Bikramjit Sharma
Asstt. Professor
Deptt. of Mechanical Engg.
Thapar University, Patiala

Countersigned by

Dr. S.K. Mohapatra
Professor & Head
Department of Mechanical Engg.
Thapar University
Patiala-147004

Dr. R.K. Sharma
Dean of Academic Affairs
Thapar University
Patiala-147004

ACKNOWLEDGEMENT

I am highly grateful to the authorities of Thapar University, Patiala for providing this opportunity to carry out the thesis work.

I would like to express a deep sense of gratitude and thank profusely to my thesis guide Sh. Bikramjit Sharma (Assistant Professor) for his sincere & invaluable guidance and suggestions which inspired me to submit thesis report in the present form.

I am highly thankful to Dr. Rahul Chibber, Dr. Ajay Batish & Dr. V.P.Agarwal for their invaluable guidance & morale boosting support from time to time.

I am also thankful to Dr. S.K. Mohapatra (H.O.D) and other faculty members and workshop staff of Mechanical Engineering Department, Thapar University, Patiala for their intellectual support. My special thanks are due to my family members and friends who constantly encouraged me to complete this work.

Sanjeev Kumar

ABSTRACT

Metal matrix composites are used mostly in space ships, aerospace, automotive, nuclear, biotechnology, electronic and sporting goods industries, but due to their high cost, experiments are usually done to reduce the cost of the composites and inexpensive materials are utilised for metal matrix composites. Fly ash is one of the most inexpensive and low density reinforcement available in large quantities as solid waste byproduct during combustion of coal in thermal power plants. So, composites with fly ash can be used to reduce the cost of the metal matrix for applications in automotive and small engine applications. It is therefore expected that the incorporation of fly ash particles in aluminium alloy will promote yet another use of this lowcost waste byproduct and at the same time has the potential for conserving energy intensive aluminium and thereby, reducing the cost of aluminium products The present research is the work on "An Experimental Study on Effects of Thermal Cycling on Cast Aluminium Composites Reinforced With Silicon Carbide And Fly Ash Particles" During this investigation, dry fly ash as received from GNDTP, Bathinda was used with Aluminium reinforced with SiC and a composite was prepared using Liquid metal stir casting route with the reducing quantity of SiC. During the research, Thermal cycling was carried out on the samples prepared and effects on samples before and after thermal cycling were observed.

LIST OF CONTENTS

`

LIST OF FIGURES

`

LIST OF TABLES

CHAPTER 1 INTRODUCTION

1.1 Composite Materials

A composite is a structural material which consists of combining two or more constituents. The constituents are combined at a microscopic level and are not soluble in each other. Other constituents is called reinforcing phase and one in which it is embedded is called the matrix. The reinforcing material may in the form of the fibres, particles or flakes. The matrix phase's materials are generally continuous. Examples of composite system include concrete reinforcement with steel, epoxy reinforced with graphite fibers etc.

Examples include wood where the lignin matrix is reinforced with cellulose fibres. Bones in which the matrix made of minerals are reinforced with collagen fibres, are also composites.

1.2 Classification of Composites

Composites are classified by the geometry of the reinforcement –Particulate, flake, and fibres –or by the type of the matrix –polymer, metal, ceramic, and carbon.

Classification of Composite Materials with Metal Matrix

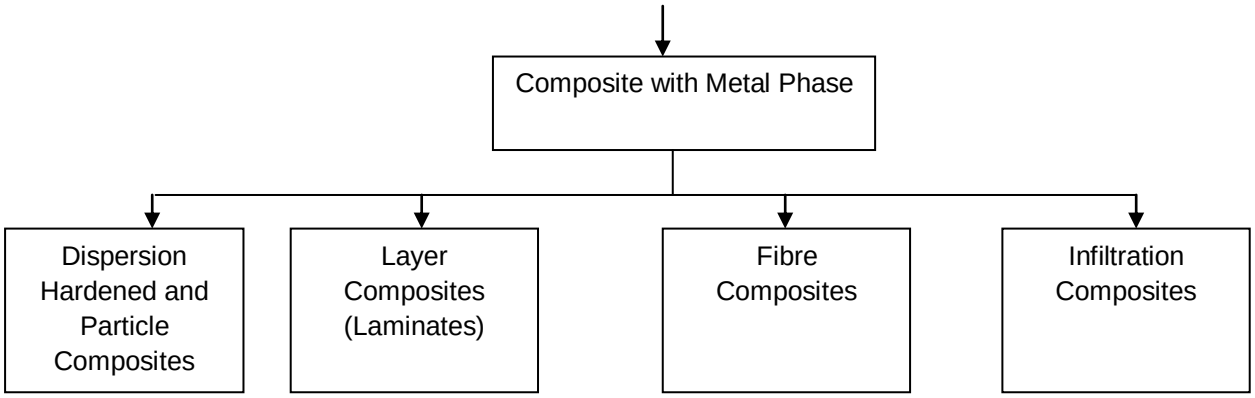

Figure 1.1- Classification of Composite Materials with Metal Matrices

Particulate composites consist of particles immersed in matrices such as alloys and ceramics. They are usually isotropic since the particles are added randomly. Particulate composites have advantages such as improved strength, increased operating temperature and oxidation resistance etc. Typical examples include use of aluminium particles in rubber, silicon carbide particles in aluminium, and gravel sand, cement to make concrete.

Flake composites consist of flat reinforcements of matrices. Typical flake materials are glass, mica, aluminium, and silver. Flake composites provide advantages such as high out-of plane flexural modulus, higher strength, and low cost. [1]

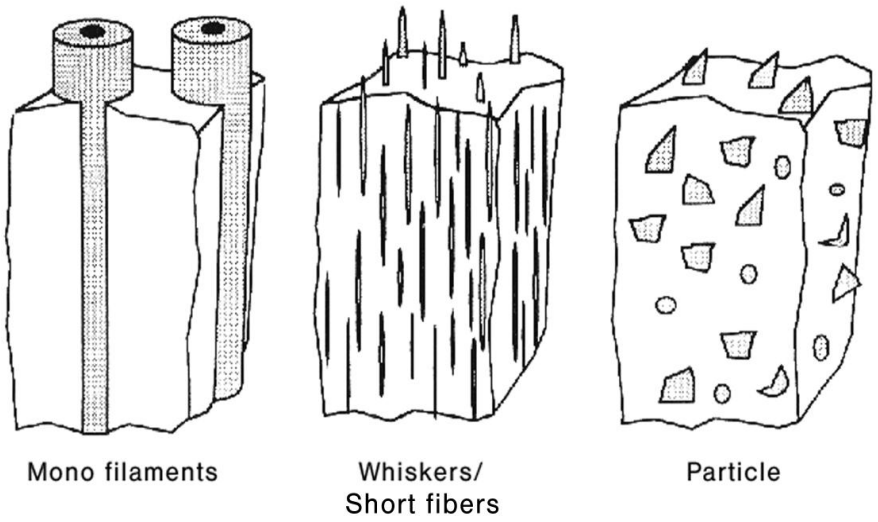

Figure 1.2 - Classifications of Composite Materials with Metal Matrices

1.2.1 Natural Composites: Several natural materials can be grouped under natural composites. e.g. bones, wood, shells, pearlite (steel which is a mixture of a phase and Fe_3C) etc.

Abalone shell ($CaCO_3$) scallop shell

Figure1.3- Natural Composite

Source: www.wikipedia.com/Composite material.html

1.2.2 Man-Made Composites: Man-made composites are produced by combining two or more materials in definite proportions under controlled conditions. e.g. Mud mixed straw to produce stronger mud mortar and bricks, Plywood, Chipboards, Decorative laminates, Fibre Reinforced Plastic (FRP), Carbon Composites, Concrete and RCC, Reinforced Glass etc.

Plywood Bricks Concrete

`

Wood Plastic Products

Wood Plastic Decking

Plastic Composite Lumber

Figure 1.4 - Man-Made Composites
Source:www.wikipedia.com/Compositematerial.html,www.bikudo.com/images/bricks

1.3 Properties of Composites

- Composites posses excellent Strength and Stiffness.
- They are very light Materials.
- They possess high resistance to corrosion, chemicals and other weathering agents. They can be moulded to any shape and size with required mechanical properties in different directions.
- High strength to weight ratio (low density high tensile strength).
- High creep resistance.
- High tensile strength at elevated temperature.

1.4 Introduction of Metal Matrix Composites

Metal Matrix Composites (MMCs), as the name implies, have a metal matrix. Examples of matrices in such composites include aluminium, magnesium, and titanium. Typical fibers include silicon and silicon carbide. Metals are mainly reinforced to increase or decrease their properties to suit the needs of design. For example, elastic stiffness and strength of metals can be increased, while large coefficients of thermal expansion and thermal and electrical conductivity of metals can be reduced by the addition of fibres such as silicon carbide.

1.5 Comparison of Composites with other Metals

Figure 1.6 below shows the comparison of metals like Steel & Aluminium with composites. The reason for choosing the aluminium and steel is that they are widely used in industry. So it can be figured out that in comparison by weight composites are much lighter than other two metals. Similarly in comparison of thermal expansion the composites are low which is good for places where high temperature working is required. In case of stiffness & strength the composites are ahead of the aluminium & steel.

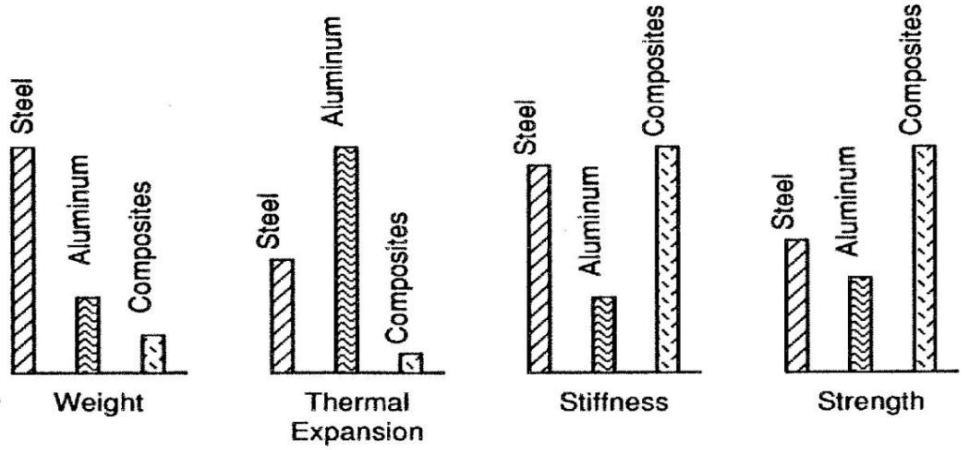

Figure 1.5 - Comparison of Composites with other Metals

1.6. Development Objectives of Metal Matrix Composites

- Increase in yield strength and tensile strength at room temperature and above while maintaining the minimum ductility or rather toughness.
- Increase in creep resistance at higher temperatures compared to that of conventional alloys, Increase in fatigue strength, especially at higher temperatures.
- Improvement of Thermal Shock Resistance.
- Improvement of Corrosion Resistance.
- Increase in Young's Modulus.
- Reduction of Thermal Elongation.

1.6.1. Manufacturing and Production of Metal Matrix Composites

Fabrication Methods for MMCs are varied .One method of manufacturing them is diffusion bonding which is used in manufacturing boron/aluminium composite parts. A fibre mat of boron is placed between two thin aluminium foils about 0.002 in. (0.005) thick. A polymer binder or acrylic adhesives holds the fibres together in the mat .Layers of these metal foils are stacked at angles as required by the design .The laminate is first heated in a vacuum bag to remove the binder .The laminate is then hot pressured with a temperature of about 932° F (500 °C) and pressure of about 5 Ksi (35 MPa) in a die to form the required machine element.

1.6.1.1. Melting Metallurgical Processes

- Infiltration of short fiber, particle or hybrid performs by casting, vacuum
- Infiltration or pressure infiltration.
- Reaction infiltration of fiber- or particle performs.
- Processing of precursor material by stirring the particles in metallic melts, followed by sand casting, permanent mold casting or high pressure die casting.

1.6.1.2. Combination of Materials for Light Metal Matrix Composites

Powder Metallurgical Processes

- Pressing and sintering and/or forging of powder mixtures and composite powders.
- Extrusion or forging of metal-powder particle mixtures.
- Extrusion or forging of spraying compatible precursor materials.
- Hot isostatic pressing of powder mixtures and fiber clutches.
- Further processing of precursor material from the melting metallurgy by thixocasting or -forming, extrusion, forging, cold massive forming or super plastic forming.
- Joining and welding of semi-manufactured products.
- Finishing by machining techniques.
- Combined deformation of metal wires (Group Superconductors)

For melting metallurgical processing of composite materials three procedures are mainly used:

- Compo-Casting or Melt Stirring Gas
- Pressure infiltration
- Pressure Casting

1.6.2 Advantages of Metal Matrix Composites

MMCs are mainly used to provide advantages over monolithic metals such as steel and aluminium.

MMCs have several advantages over the polymer composites. These include higher elastic properties, higher service temperature, insensitivity to moisture, higher electrical and thermal conductivities, and better wear fatigue, and flaw resistances. The drawbacks of MMCs over PMCs include higher processing temperature and higher densities.

- Dimensional stability (e.g. Space based telescope)
- Low dielectric
- Corrosion resistance
- Aero Elastic Tailoring
- Weight Saving

1.6.3 Matrix Materials and Key Composites

1.6.3.1. Aluminium Matrix

- Continuous Fibres : Boron ,Silicon Carbide, Alumina, Graphite
- Discontinuous Fibres : Alumina, Alumina-Silica
- Whiskers : Silicon Carbide
- Particulates : Silicon Carbide, Boron Carbide

Matrices of Aluminium Matrix Composites are usually based on aluminium-silicon (Al-Si) alloys and on the alloys of 2xxx and 6xxx series.

Aluminium Matrix Composites (AMC) are reinforced by:

- Alumina (Al_2O_3) or silicon carbide (**SiC**) particles (particulate Composites) in amounts 15-70 vol%;
- Continuous fibers of alumina, silicon carbide, Graphite (long-fiber reinforced composites);
- Discontinuous fibers of alumina (short-fiber reinforced composites);

Aluminium Matrix Composites are manufactured by the following fabrication methods:

- Powder Metallurgy(Sintering);
- Stir Casting;
- Infiltration;

The following properties are typical for Aluminium Matrix Composites:

- High strength even at Elevated Temperatures;
- High stiffness (Modulus of Elasticity);
- Low Density;
- High Thermal Conductivity;
- Excellent Abrasion Resistance.

Aluminium Matrix Composites (AMC) are used for Manufacturing of Automotive Parts (Pistons, Pushrods, and Brake Components), Brake Rotors for high speed trains, bicycles, golf clubs, electronic substrates, cores for high voltage electrical cables.

1.6.3.2 Magnesium Matrix

- Continuous Fibres : Graphite, Alumina
- Whiskers : Silicon Carbide
- Particulates : Silicon Carbide, Boron Carbide

Magnesium Matrix Composites are reinforced mainly by silicon carbide (**SiC**) particles (particulate composites).

The following properties are typical for Magnesium Matrix Composites:

- Low density;
- High Stiffness (modulus of elasticity);
- High wear resistance;
- Good Strength even at elevated temperatures;
- Good Creep resistance.

Magnesium Matrix Composites are used for manufacturing components for racing cars, lightweight automotive brake system, and aircraft parts for: gearboxes, transmissions, compressors and engine.

1.6.3.3 Titanium Matrix

`

- Continuous Fibres: Graphite, Silicon Carbide.
- Wires: niobium-titanium, niobium-tin.
- Particulates: Silicon Carbide, Boron Carbide, Titanium Carbide.

Titanium Matrix Composites are reinforced mainly by:

- Continuous monofilament silicon carbide fiber (long-fiber reinforced composites);
- Titanium boride (**TiB_2**) and titanium carbide (**TiC**) particles (particulate composites).

Powder metallurgy (sintering) is used for fabrication of Titanium Matrix Composites.

The following properties are typical for Titanium Matrix Composites:

- High strength;
- High stiffness (modulus of elasticity);
- High creep resistance;
- High thermal stability;
- High wear resistance.

Titanium Matrix Composites are used for manufacturing structural components of the F-16 jet's landing gear, turbine engine components (fan blades, actuator pistons, synchronization rings, connecting links, shafts, and discs), automotive engine components, drive train parts, general machine components.

1.6.3.4 Super alloy Matrices

- Wires : Tungsten

1.6.3.5 Copper Matrix Composites

Copper Matrix Composites are reinforced by:

- Continuous fibres of carbon (**C**), silicon carbon (**SiC**), tungsten (**W**), stainless steel 304 (long-fibre reinforced composites);
- Silicon carbide particles (particulate composites).

Powder metallurgy (sintering) and infiltration technique are used for fabrication Copper Matrix Composites.

The following properties are typical for Copper Matrix Composites:

- Low coefficient of thermal expansion;
- High stiffness (modulus of elasticity);
- Good electrical conductivity;
- High thermal conductivity;

- Good wear resistance.

Copper Matrix Composites are used for manufacturing hybrid modules, electronic relays, electrically conducting springs and other electrical and electronic components. [2]

1.6.4. Typical Mechanical Properties of Some Metal Matrix Composites Typical mechanical properties of MMCs are given in Table -1.1 as shown below (System of Units: SI):

Table 1.1 - Typical mechanical properties of MMCs

Property	Units	SiC/ Aluminium	Graphite /Aluminium	Steel	Aluminium
Specific Gravity	Nil	2.6	2.2	7.8	2.6
Young's Modulus	GPa	117.2	124.1	206.8	68.95
Ultimate Tensile Strength	MPa	1206	448.2	648.1	234.40
Coefficient of Thermal Expansion	Mm/m/°C	12.4	18	11.7	23

1.6.5 Disadvantages of Metal Matrix Composites

- High Production Cost
- Difficult to Repair
- Susceptible to Damage

1.6.6 Uses of Metal Matrix Composites

- Extensively used in space technology and production of *Aerospace components* (tails, wings, fuselages, propellers).
- Used in the production of sport goods e.g. *racing car* bodies and *bicycle frames* etc.
- Used for general industrial and engineering structures.
- Used in high speed and fuel efficient transport vehicles.
- The shell composed of Cosmo Lite, a thermoplastic fibre-reinforced composite and the exterior surface Spectra Lite which incorporates DuPont Surlyn, an impact-resistant coating found on *golf balls.*
- Carbon composite is a key material in today's launch vehicles and spacecraft. It is widely used in solar panel substrates, antenna reflectors and yokes of spacecraft. It is also used in payload adapters, inter-stage structures and heat shields of launch vehicles.

`

1.7 Production of Metal Matrix Composites by Stir Casting

Liquid state fabrication of Metal Matrix Composites involves incorporation of dispersed phase into a molten matrix metal, followed by its Solidification. In order to provide high level of mechanical properties of the composite, good interfacial bonding (wetting) between the dispersed phase and the liquid matrix should be obtained.
Wetting improvement may be achieved by coating the dispersed phase particles (fibers). Proper coating not only reduces interfacial energy, but also prevents chemical interaction between the dispersed phase and the matrix.
The simplest and the most cost effective method of liquid state fabrication is Stir Casting.

1.7.1 Stir Casting

Stir Casting is a liquid state method of composite materials fabrication, in which a dispersed phase (ceramic particles, short fibers) is mixed with a molten matrix metal by means of mechanical stirring. The liquid composite material is then cast by conventional casting methods and may also be processed by conventional Metal forming technologies.
Stir Casting is characterized by the following features:

- Content of dispersed phase is limited (usually not more than 30 vol. %).
- Distribution of dispersed phase throughout the matrix is not perfectly homogeneous.
- Distribution of dispersed phase may be improved if the matrix is in semi-solid condition. The method using stirring metal composite materials in semi-solid state is called Rheocasting.
- High viscosity of the semi-solid matrix material enables better mixing of the dispersed phase.

1.8 Fly Ash

Metal matrix composites (MMCs) possess significantly improved properties including high specific strength; specific modulus, damping capacity and good wear resistance compared to unreinforced alloys. There has been an increasing interest in composites containing low density and low cost reinforcements. Among various discontinuous dispersoids used, fly ash is one of the most inexpensive and low density reinforcement available in large quantities as solid waste by-product during combustion of coal in thermal power plants. Hence, composites with fly ash as reinforcement are likely to overcome the cost barrier for wide spread applications in automotive and small engine applications. It is therefore expected that the incorporation of fly ash particles in aluminum alloy will promote yet another use of this low-cost waste by-product and, at the same time, has the potential for conserving energy intensive aluminum and thereby, reducing the cost of aluminum products. Now a days the particulate reinforced aluminum matrix composite are gaining importance because of their low cost with advantages like isotropic properties and the possibility of secondary processing facilitating fabrication of secondary components. The present investigation has been focused on the utilization of abundantly available industrial waste fly-ash in useful manner by dispersing it into aluminum to produce composites by stir casting method.

Fly ash is one of the residues generated in the combustion of coal. Fly ash is generally captured from the

chimneys of coal-fired power plants, and is one of two types of ash that jointly are known as coal ash; the other, bottom ash, is removed from the bottom of coal furnaces. Depending upon the source and makeup of the coal being burned, the components of fly ash vary considerably, but all fly ash includes substantial amounts of silicon dioxide (SiO_2) (both amorphous and crystalline) and calcium oxide (CaO), both being endemic ingredients in many coal bearing rock strata.

Toxic constituents depend upon the specific coal bed makeup, but may include one or more of the following elements or substances in quantities from trace amounts to several percent: arsenic, beryllium, boron, cadmium, chromium, chromium VI, cobalt, lead, manganese, mercury, molybdenum, selenium, strontium, thallium, and vanadium, along with dioxins and PAH compounds.

In the past, fly ash was generally released into the atmosphere, but pollution control equipment mandated in recent decades now requires that it be captured prior to release. In the US, fly ash is generally stored at coal power plants or placed in landfills. About 43 percent is recycled, often used to supplement Portland cement in concrete production. Some have expressed health concerns about this. Fly ash is increasingly finding use in the synthesis of geopolymers and zeolites.

1.8.1 Chemical Composition and Classifications

Fly ash material solidifies while suspended in the exhaust gases and is collected by electrostatic precipitators or filter bags. Since the particles solidify while suspended in the exhaust gases, fly ash particles are generally spherical in shape and range in size from 0.5 µm to 100 µm. They consist mostly of silicon dioxide (SiO_2), which is present in two forms: amorphous, which is rounded and smooth, and crystalline, which is sharp, pointed and hazardous; aluminium oxide (Al_2O_3) and iron oxide (Fe_2O_3). Fly ashes are generally highly heterogeneous, consisting of a mixture of glassy particles with various identifiable crystalline phases such as quartz, mullite, and various iron oxides.

Table 1.2.- Contents in Fly Ash

Component	Bituminous	Sub-Bituminous	Lignite
SiO_2 (%)	20-60	40-60	15-45
Al_2O_3 (%)	5-35	20-30	20-25
Fe_2O_3 (%)	10-40	4-10	4-15
CaO (%)	1-12	5-30	15-40
LOI (%)	0-15	0-3	0-5

Fly ash also contains environmental toxins in significant amounts, including arsenic (43.4 ppm); barium (806 ppm); beryllium (5 ppm); boron (311 ppm); cadmium (3.4 ppm); chromium (136 ppm); chromium VI (90 ppm); cobalt (35.9 ppm); copper (112 ppm); fluorine (29 ppm); lead (56 ppm); manganese (250 ppm); nickel (77.6 ppm); selenium (7.7 ppm); strontium (775 ppm); thallium (9 ppm); vanadium (252 ppm); and zinc (178 ppm).

`

Two classes of fly ash are defined by ASTM C618: Class F fly ash and Class C fly ash. The chief difference between these classes is the amount of calcium, silica, alumina, and iron content in the ash. The chemical properties of the fly ash are largely influenced by the chemical content of the coal burned (i.e., anthracite, bituminous, and lignite).

Not all fly ashes meet ASTM C618 requirements, although depending on the application, this may not be necessary. Ash used as a cement replacement must meet strict construction standards, but no standard environmental standards have been established in the United States. 75% of the ash must have a fineness of 45 µm or less, and have carbon content, measured by the loss on ignition (LOI), of less than 4%. In the U.S., LOI needs to be fewer than 6%. The particle size distribution of raw fly ash is very often fluctuating constantly, due to changing performance of the coal mills and the boiler performance. This makes it necessary that fly ash used in concrete needs to be processed using separation equipment like mechanical air classifiers. Especially important is the ongoing quality verification. This is mainly expressed by quality control seals like the Bureau of Indian Standards mark or the DCL mark of the Dubai Municipality.

1.8.1 Class F Fly Ash

The burning of harder, older anthracite and bituminous coal typically produces Class F fly ash. This fly ash is pozzolanic in nature, and contains less than 10% lime (CaO). Possessing pozzolanic properties, the glassy silica and alumina of Class F fly ash requires a cementing agent, such as Portland cement, quicklime, or hydrated lime, with the presence of water in order to react and produce cementitious compounds. Alternatively, the addition of a chemical activator such as sodium silicate (water glass) to a Class F ash can lead to the formation of a geopolymer.

1.8.2 Class C Fly Ash

Fly ash produced from the burning of younger lignite or subbituminous coal, in addition to having pozzolanic properties, also has some self-cementing properties. In the presence of water, Class C fly ash will harden and gain strength over time. Class C fly ash generally contains more than % lime (CaO). Unlike Class F, self-cementing Class C fly ash does not require an activator. Alkali and sulfate (SO_4) contents are generally higher in Class C fly ashes.

At least one US manufacturer has announced a fly ash brick containing up to 50 percent Class C fly ash. Testing shows the bricks meet or exceed the performance standards listed in ASTM C 216 for conventional clay brick; it is also within the allowable shrinkage limits for concrete brick in ASTM C 55, Standard Specification for Concrete Building Brick. It is estimated that the production method used in fly ash bricks will reduce the embodied energy of masonry construction by up to 90%.

1.8.3 Disposal and Market Sources

In the past, fly ash produced from coal combustion was simply entrained in flue gases and dispersed into the atmosphere. This created environmental and health concerns that prompted laws which have reduced

fly ash emissions to less than 1% of ash produced. Worldwide, more than 65% of fly ash produced from coal power stations is disposed of in landfills and ash ponds. In India alone, fly ash landfill covers an area of 40,000 acres (160 km^2).

1.8.4 Fly Ash Reuse

The reuse of fly ash as an engineering material primarily stems from its pozzolanic nature, spherical shape, and relative uniformity. Fly ash recycling, in descending frequency, includes usage in:

- Portland Cement and Grout
- Embankments and Structural fill
- Waste Stabilization and Solidification
- Raw feed for Cement Clinkers
- Mine Reclamation
- Stabilization of Soft Soils
- Road Subbase
- Aggregate
- Flowable fill
- Mineral filler in Asphaltic Concrete
- Other applications include cellular concrete, geopolymers, roofing tiles, paints, metal castings, and filler in wood and plastic products.

  For this theses work, the Dry fly ash has been taken from Guru Nanak Dev Thermal Power Plant, Bathinda and with the following constituents

Doc. No. :- F-Q040-04

Chemical Testing Of Dry Fly Ash (Weekly)

Month :-Jan.- 10 FROM :-CNDTP (FTL)

Date Of Receipt	Chemical Analysis								Total Alaklis
	LOI	IR	So3	Sio2	Al2O3	Fe2O3	CaO	MgO	
03/01/10 TO 09/01/10	1.62	92.48	0.09	58.16	27.24	5.24	1.94	0.71	1.01
10/01/10 TO 16/01/10	1.35	93.73	0.08	58.11	27.19	5.21	1.96	0.72	1.00
17/01/10 TO 23/01/10	1.27	93.31	0.08	58.17	27.22	5.23	2.00	0.70	1.01
24/01/10 TO 30/01/10	1.14	93.02	0.09	58.20	27.21	5.22	1.98	0.71	1.00
	1.35	93.14	0.09	58.16	27.22	5.23	1.97	0.71	1.01

Table 1.3 Constituents of Dry Flyash

Doc. No. :- F-Q040-03

Month :Jan.-2010 DRY FLY ASH ANALYSIS FROM :GNDTP [BTI]

DATE	LOI	IR	Specific Surface	+45 MICRONS RESIDUE	+90 MICRONS RESIDUE	+210 MICRONS RESIDUE	Specific Surface	LIME REACTIVITY
01. Jan 10	1.34	93.56	3721	27.10	7.14	0.74		
02. Jan 10	1.73	92.93	3674	28.16	7.70	0.92		
03. Jan 10	1.56	92.80	3702	26.94	6.92	0.78		
04. Jan 10	1.81	93.75	3640	27.90	7.10	0.70		
05. Jan 10	1.88	93.85	3648	27.78	7.24	0.68		
06. Jan 10	1.50	92.96	3547	28.24	7.76	0.88		
07. Jan 10	1.64	92.21	3649	28.02	7.58	0.74	3644	54.00
08. Jan 10	1.07	92.81	3545	28.32	7.82	0.96		
09. Jan 10	1.33	92.65	3765	27.76	7.48	0.64		
10. Jan 10	1.23	93.02	3721	27.84	7.60	0.76		
11. Jan 10	1.20	93.71	3640	27.96	7.78	0.86		
12. Jan 10	1.51	93.81	3556	28.12	7.50	0.78		
13. Jan 10	1.45	94.04	3610	27.80	7.64	0.62		
14. Jan 10	1.29	94.27	3712	27.48	7.52	0.56	3702	53.00
15. Jan 10	1.70	93.43	3658	27.70	7.92	0.64		
16. Jan 10	1.05	93.21	3894	24.10	6.80	0.48		
17. Jan 10	1.14	93.09	3882	22.90	5.44	0.46		
18. Jan 10	1.06	93.58	3740	23.70	5.90	0.42		
19. Jan 10	1.24	94.30	3744	24.16	6.10	0.42		
20. Jan 10	1.36	93.47	3707	24.10	6.16	0.40		
21. Jan 10	1.45	93.72	3740	23.88	6.24	0.48	3724	55.00
22. Jan 10	1.58	93.22	3702	23.56	6.40	0.54		
23. Jan 10	1.24	93.37	3849	23.24	6.20	0.58		
24. Jan 10	1.38	93.01	3902	23.02	5.88	0.48		
25. Jan 10	1.02	94.18	4015	22.74	5.44	0.40		
26. Jan 10	1.12	92.95	4085	22.98	5.70	0.42		
27. Jan 10	0.98	93.72	4019	23.26	5.98	0.46		
28. Jan 10	1.07	93.52	4002	23.34	6.10	0.58	3875	53.00
29. Jan 10	1.01	93.36	3987	23.96	6.42	0.44		
30. Jan 10	1.18	93.61	3779	24.40	6.64	0.60		
31. Jan 10	1.14	93.47	3804	24.28	6.44	0.54		
MIN.	**0.98**	**92.21**	**3545**	**22.74**	**5.44**	**0.40**	**3644**	**53.00**
MAX.	**1.88**	**94.30**	**4085**	**28.32**	**7.92**	**0.96**	**3875**	**55.00**
AVG.	**1.33**	**93.41**	**3763**	**25.64**	**6.79**	**0.61**	**3736**	**53.75**

Dec 10

`

1.8.6 Calculation of Grain fineness number of Dry Fly Ash

Grain fineness number of the Dry Fly ash received was found out as given in the table below:

Table 1.3 – Calculation of Grain Fineness Number

Sr.No. (a)	Multiplying factor (b)	Amount of Flyash retained(9M) (c)	Flyash % retained (d)	Product e=(d)x(b)
8	6	0	0	0
10	8	0	0	0
16	10	0	0	0
22	16	0	0	0
30	22	0.93	1.86	40.92
44	30	1.09	2.18	65.40
60	44	0.16	0.32	14.08
100	60	3.22	6.44	386.40
150	100	23.31	46.62	4662
200	150	15.58	31.16	4674
300	200	2.89	5.78	1156
PAN		$\sum c$= 47.18	$\sum d$ =94.76	10,998.80

Average Gain Fineness Number $\sum e/\sum d$ = 10998.80/ 94.76 = 116.56

Average GFN = 50.26

1.9 Measurement of Thermal Conductivities

1.9.1 Measurement of Thermal Conductivities of Dry Fly Ash

To find the thermal conductivity experiments were carried out using apparatus available in heat transfer lab.The holdup consists of two thin walled concentric spheres of different diameters and made out of copper sheet. The insulating material or powder is packed tightly, between these two spheres in a manner such that there are no air gaps left in the insulating material as well as between the powder and sphere walls. The inner sphere is provided with a heat source in the form of an electrical resistance coil. The input to the heat source is measured with the help of a voltmeter and ammeter. Further, by providing variac in the circuitry of heating coil, the input can be varied. For the measurement of temperature chromal-alumel thermocouple have been employed. Thermocouple numbered TC1 to TC4 are embedded on the outer surface of the inner sphere. Equidistantly for arising out at the an average temperature of the inner sphere, whereas the thermocouple involved in humbled TC5 to TC10 are embedded on the inner surface of the outer sphere equidistantly for arising out at the average temperature of the outer sphere, Readings of thermocouples attached with the spheres were noted down and readings were taken at an interval of 30 Minutes and thermal conductivity was found out as described below:

Radius of the inner sphere Ri = 50 mm

Radius of the outer sphere Ro = 100 mm

Voltmeter Reading, V = 31.2V

Ammeter Reading, I = 0.421A

Heat Input (Q) = V*I = 132 W

Inner Sphere

Sr.No.	Time	Temperature of thermocouple				Average temperature ,T1(^{o}C)
		TC1 (^{o}C)	TC2(^{o}C)	TC3(^{o}C)	TC4(^{o}C)	
1	11.50	17	17	17	17	17
2	12.20	32	32	32	32	32
3	12.50	46	46	46	46	46
4	1.20	48	48	48	48	48
5	1.50	55	55	55	55	55
6	2.20	57	57	57	57	57

Outer Sphere

Radius of the inner sphere, = 50mm

Radius of the outer sphere = 100mm

Voltmeter reading V =0.422 V

Ammeter Reading I=32 A

Sr.No.	Time	Temperature of thermocouple						Average temperature ,T1(^{o}C)
		TC5 (^{o}C)	TC6(^{o}C)	TC7(^{o}C)	TC8(^{o}C)	TC9(^{o}C)	TC10(^{o}C)	
1.	11.50	17	17	17	17	17	17	17
2,	12.20	32	32	32	32	32	32	32
3.	12.50	46	46	46	46	46	46	46
4.	1.20	48	48	48	48	48	48	48
5.	1.50	55	55	55	55	55	55	55
6.	2.20	57	57	57	57	57	57	57

Thermal Conductivity = 0.033 Watt/m-K

`

1.12.2 Measurement of Thermal conductivity of SiC

To find out the thermal conductivity of SiC, same procedure as that of fly ash was used and the results are as below:

Radius of the inner sphere Ri, = 50mm

Radius of the outer sphere ,Ro =100mm

Voltmeter Reading, V =33.1V

Ammeter Reading, I =0.461 A

Heat Input (Q) = V*I = 15.26 W

Inner Sphere

Sr.No.	**Time**	**Temperature of thermocouple**				**Average temperature ,T1(^oC)**
		TC1 (^oC)	TC2(^oC)	TC3(^oC)	TC4(^oC)	
1.	10.40	18	18	18	18	18
2,	11.10	22	22	22	22	22
3.	11.40	26	26	26	26	26
4.	12.10	29	27	28	-	28
5.	12.40	29	28	29	-	28.66

Outer Sphere

Voltmeter reading V =33.6 V

Ammeter Reading I=0.272 A

Sr.No.	**Time**	**Temperature of thermocouple**						**Average temperature ,T1(^oC)**
		TC5 (^oC)	TC6(^oC)	TC7(^oC)	TC8(^oC)	TC9(^oC)	TC10(^oC)	
1.	10.40	18	18	18	18	18	18	18
2,	11.10	22	22	22	22	22	22	22
3.	11.40	26	26	26	26	26	26	26
4.	12.10	41	23	23	23	21	23	25.66
5.	12.40	37	21	22	21	20	22	23.83

Thermal Conductivity = 0.909 Watt/m-K

`

1.10. X-Ray Powder Diffraction

X-ray powder diffraction (XRD), is an instrumental technique that is used to identify minerals, as well as other crystalline materials. XRD provides the researcher with a fast and reliable tool for routine mineral identification. XRD is particularly useful for identifying finegrained minerals and mixtures or intergrowths of minerals that may not lend themselves to analysis by other techniques. XRD can provide additional information beyond basic identification. If the sample is a mixture, XRD data can be analyzed to determine the proportion of the different minerals present. Other information obtained can include the degree of crystalline of the mineral(s) present, possible deviations of the minerals from their ideal compositions (presence of element substitutions and solid solutions), the structural state of the minerals (which can be used to deduce temperatures and (or) pressures of formation), and the degree of hydration for minerals that contain water in their structure. Some mineralogical samples analyzed by XRD are too fine grained to be identified by optical light microscopy.XRD does not, however, provide the quantitative compositional data obtained by the electron microprobe or me textural and qualitative compositional data obtained by the scanning electron microscope.

Theory and Methodology of XRD

The three-dimensional structure of nonamorphous materials, such as minerals, is defined by regular, repeating planes of atoms that form a crystal lattice. When a focused X-ray beam interacts with these planes of atoms, part of the beam is transmitted, part is absorbed by the sample, part is refracted and scattered, and part is diffracted. Diffraction of an X-ray beam by a crystalline solid is analogous to diffraction of light by droplets of water, producing the familiar rainbow. X-rays are diffracted by each mineral differently, depending on what atoms make up the crystal lattice and how these atoms are arranged. In X-ray powder diffractometry+9, X-rays are generated within a sealed tube that is under vacuum. A current is applied that heats a filament within the tube, the higher the current the greater the number of electrons emitted from the filament. This generation of electrons is analogous to the production of electrons in a television picture tube. A high voltage, typically 15-60 kilovolts, is applied within the tube. This high voltage accelerates the electrons, which then hit a target, commonly made of copper. When these electrons hit the target, X-rays are produced. The wavelength of these X rays is characteristic of that target. These X-rays are collimated and directed onto the sample, which has been ground to a fine powder (typically to produce particle sizes of less than 10 microns). A detector detects the X-ray signal; the signal is then processed either by a microprocessor or electronically, converting the signal to a count rate. Changing the angle between the X-ray source, the sample, and the detector at a controlled rate between preset limits is an X-ray scan. When an X-ray beam hits a sample and is diffracted, we can measure the distances between the planes of the atoms.

`

1.11 Scanning Electron Microscope (SEM)

The scanning electron microscope (SEM) is a type of electron microscope that images the sample surface by scanning it with a high-energy beam of electrons in a raster scan pattern. The electrons interact with the atoms that make up the sample producing signals that contain information about the sample's surface topography, composition and other properties such as electrical conductivity.

The types of signals produced by an SEM include secondary electrons, back-scattered electrons (BSE), characteristic X-rays, light (cathodoluminescence), specimen current and transmitted electrons. Secondary electron detectors are common in all SEMs, but it is rare that a single machine would have detectors for all possible signals. The signals result from interactions of the electron beam with atoms at or near the surface of the sample. In the most common or standard detection mode, secondary electron imaging or SEI, the SEM can produce very high-resolution images of a sample surface, revealing details about less than 1 to 5 nm in size. Due to the very narrow electron beam, SEM micrographs have a large depth of field yielding a characteristic three-dimensional appearance useful for understanding the surface structure of a sample. This is exemplified by the micrograph of pollen shown to the right. A wide range of magnifications is possible, from about 10 times (about equivalent to that of a powerful hand-lens) to more than 500,000 times, about 250 times the magnification limit of the best light microscopes.

`

CHAPTER 2 LITERATURE REVIEW

N. L. Han, Z. G. Wanget et al. [4] study the Low-Cycle Fatigue behaviour of a Particulate SiC/2024Al composite at ambient and elevated temperature and its unreinforced matrix alloy at 22 and 190°C. The test results showed that the cyclic stress response characteristics of the composite and the 2024Al alloy were similar to each other in spite of changing the test temperature.

RCéline A. Mahieux et al.[5] have studied the effect of temperature on polymer matrix composites.Mechanical, electrical and optical properties can undergo order of magnitude changes over a 100°C temperature change and moisture diffusion can vary by as much as three orders of magnitude. Generally speaking, the re-arrangement rate increases with temperature.

Rajendra U Vaidya et al. [6] studied the thermal expansion of various fiber- and particle-reinforced metal-matrix composites has been measured and the experimentally obtained values compared with the predictions of various theoretical models. The particulate composites exhibited some residual strain when cooled down from the peak temperature to room temperature. The magnitude of this strain was a function of the peak temperature and number of thermal cycles. These composites exhibited very small residual strains when cooled down from the peak temperature to room temperature. In addition, the thermal expansion response was not linear over the test temperature range but exhibited regions of distinctly different slopes.

Elhem Ghorbel et al.[7] investigated the Interface degradation in metal-matrix composites under cyclic thermo-mechanical loading. Thermal cycles under constant load have been performed on [±45] C/Al and SiC/Al composites. Effects of temperature amplitude and tensile stress levels were investigated to improve the design of metal-matrix composites structures and to prevent their failure. When submitted to thermal cycling under constant loads, both composites exhibit a progressive plastic deformation which increases with the number of cycles, even at stress levels far below the yield stress. This phenomenon, related to thermal ratchetting, is expressed as a function of both the applied stress and the amplitude of thermal cycles by a power creep law. The duration of exposure at the highest temperature of the thermal cycle does not play a significant role in determining the ratchetting rate. SEM observations show reaction products at the surfaces of the fibers. However, it appears that the main phenomenon leading to composite failure is ratchetting for high load levels and interface degradation for low load levels.

Tran Huu Nam et al. **[8]** have investigated the Thermal Expansion behaviour of aluminium matrix composites with densely packed SiC particles. The coefficient of thermal expansion (CTE) of Al-based metal matrix composites containing 70 vol. % SiC particles (AlSiC) has been measured based on the length change from room temperature (RT) to 500 °C. In the work, this instantaneous CTE (T) of AlSiC is studied by thermo-elastic models and micromechanical simulation using finite element analysis. . The CTE (T) is modelled for heating and cooling cycles from 20 °C to 500 °C considering the effects of microscopic voids and phase connectivity. The thermal expansion behaviour is strongly influenced by the presence of voids and confirms qualitatively that they cause the experimentally observed decrease of the CTE (T) above 250 °C.

`

S. Elomari et al. [9] have studied the Thermal Expansion behaviour of particulate metal-matrix composites. Aluminium-matrix composites containing thermally oxidized SiC particles of controlled diameter ranging from 3 to 40 μm have been produced successfully by vacuum assisted high-pressure infiltration. Their thermal-expansion coefficients (CTEs) were measured between 25 and 500 °C with a high-precision thermal mechanical analyser (TMA), and compared with the predictions of various theoretical models.

Y. C. Qin, S. Y.He et al. [10] studied the Effect of thermal–mechanical cycling on thermal expansion behaviour of boron fiber-reinforced aluminium matrix composite. The thermal expansion behaviour of boron fiber-reinforced aluminium matrix composite subjected to thermal–mechanical cycling (TMC) was studied. Experimental results showed that TMC affected greatly the thermal expansion behaviour of the composite. Using a simple analysis model of internal stress in the fibers, the stress change during the thermal expansion coefficient measurements of the composite subjected to TMC was calculated. The results indicated that TMC could induce the interfacial degradation of the composite, and the more the numbers of TMC cycles, or the higher the applied stress level of TMC, the more serious the interfacial degradation of the composite became. The proposed one-dimensional analysis model was proved to be a simple and qualitative approach to probing the interfacial degradation of unidirectional fiber-reinforced metal matrix composites during TMC.

S. Hertz-Clemens et al.[11] studied the Damage mechanisms under thermal-Mechanical fatigue in a unidirectionally reinforced SiC-titanium metal matrix composite for advanced jet engine components. The thermal-mechanical fatigue behaviour of a titanium composite reinforced by continuous SiC fibres, the SM 1140+/Ti-6242, was investigated for uniaxial loading, under conditions which simulate service loading in a compressor disc during a flight. The thermal-mechanical tests (100–500°C) give rise to a reduction of fatigue lives compared to isothermal tests (550°C).

S. Q. Wu, Z. S et al. [12] studied the mechanical and thermal expansion behaviour of an Al–Si alloy composite reinforced with potassium titanate whisker. Composites of aluminium–silicon (Al–12 wt. %Si) alloy reinforced with potassium titanate whiskers were prepared by the squeeze casting process. Strain hysteresis was observed in Al–12Si alloy and its composites subjected to thermal cycling. The thermal response curves indicated that the Al–12Si alloy exhibits the largest thermal and residual plastic strains subjected to heating and cooling cycles between 50 and 280°C.

H. Mykura et al. [13] have studied the Thermal Expansion and stress relaxation of metal-matrix composites. The coefficient of thermal expansion (CTE) of a series of Al-6%Si matrix samples, with reinforcements of carbon, SiC, Al_2O_3, or boron fibres, cloths, or ceramic particles was measured in the range 60°–220°C with a dilatometer.

A.R.S. Ponter et al.[14] have studied the bounding properties of metal-matrix composites subjected to cyclic thermal loading. The paper is concerned with the load-bearing capacity of a body with a regular periodic microstructure with elastic and elastic-perfectly plastic phases, such as a metal-matrix composite, when subjected to cyclic thermal loading.

A. R. S. Ponter et al. [15] have studied the on the behaviour of metal matrix composites subjected to cyclic thermal loading. The mechanical properties of metal matrix composite materials are strongly

affected by thermal cycling. Through the study of experimental data, for an aluminium / alumina continuous fibre composite, the paper investigates the relationship between the observed behaviour and the predictions, using simplified methods of analysis, of classical plasticity models for the matrix material.

N. L. Han et al. [16] studied the effect of reinforcement size on the elevated-temperature tensile properties and low-cycle fatigue behaviour of particulate SiC/Al composites. The cyclic stress response characteristics and low-cycle fatigue endurance of powder-metallurgy-processed commercially pure aluminium composites reinforced with SiC particles of different sizes and of the unreinforced matrix were studied under a range of cyclic plastic strains at 441 K. At elevated temperature the composites and unreinforced aluminium alloy definitely show cyclic softening.

S. Jansson et al. [17] studied the Transverse and Cyclic thermal loading of the fiber reinforced metal-matrix composite SCS6/Ti-15-3. The transverse properties of a SiC fiber reinforced Ti alloy matrix composite subjected to transverse mechanical and cyclic thermal loading have been investigated. Fibers and matrix have a mismatch in the coefficients of thermal expansion that induces thermal stresses in addition to those caused by mechanical loading.

W.A. Uju et al. [18] studied the Thermal cycling behaviour of stir cast Al–Mg alloy reinforced with fly ash. The thermal cycling behaviour of stir cast Al–Mg alloy A535 composites reinforced with various amounts of fly ash was investigated in this study. The test samples were subjected to 10 thermal cycles between 40 and 300 °C. The results show that strain hysteresis loops developed during thermal cycling. The hysteresis and residual plastic strains induced in the alloy during thermal cycling decreased with the addition of fly ash. Also, the incorporation of fly ash in A535 improved its dimensional stability.

M. J. Tan et al. [19] have studied the Thermal Cycling processes in metal-matrix composites. In this work, a study of the behaviour of AA6061 reinforced with alumina particles produced by casting and extrusion, under the action of strain control and thermal cycling conditions, is presented. Comparisons are made with unreinforced AA6061 matrix, and also with the same composite re-extruded to obtain finer grain sizes. Elongations obtained via thermal cycling are compared with those from room temperature and isothermal testing. The work also looks at the differences in cycling at different frequencies, range and rate, for the AA6061 matrix composites.

Y.D. Huang et al. [20] investigated on Investigated on thermal fatigue of aluminium- and magnesium-alloy based composites. Both the KS1275® piston and AE42 alloys and their composites have realistic and/or potential applications as engine components in the automotive industry. Used as engine components, the dimensional stability is of great concern. Thermal cycling experiments can simulate the service conditions of the materials and give an evaluation how the dimension changes during their service in the changing temperature environments. The present paper investigates the thermal fatigue of the short fiber reinforced KS1275® piston and AE42 alloys, with an emphasis on the changes in the strain and hardness before and after thermal cycling.

Z. R. Xu et al. [21] studied the stiffness loss and density decrease due to thermal cycling in an alumina fiber/magnesium alloy composite. Thermal expansion mismatch between a ceramic reinforcement and a

metallic matrix can lead to thermal stresses under cyclic temperature conditions. This can lead to plastic deformation of the ductile metallic matrix, void formation at the reinforcement/matrix interface, and possible fracture of the reinforcement. Stiffness and density were used as damage parameters to study damage evolution as a function of thermal cycles in a unidirectional, continuous alumina fiber Al_2O_{3f}/ZE41A Mg alloy composite. Specimens were thermally cycled up to 3000 cycles between room temperature (22 °C) and 300 °C. The incidence of void formation increased with the number of cycles. Stiffness and density of this composite decreased with thermal cycling.

Y. D. Huang et al. [22] studied the thermal behaviour of short fiber reinforced AlSi12CuMgNi piston alloys. This work investigated both the aging and thermal cycling behaviours of the short fiber reinforced AlSi12CuMgNi piston alloys using X-ray diffraction, microhardness and thermal dilatometry tests. The magnesium is essential for the formation of strengthening precipitates, but it could deplete due to its reaction with the SiO_2 in the fiber or in the binder, and therefore the age hardening could be suppressed. The coefficient of thermal expansion (CTE) is affected by both the microstructure and internal thermal stresses generated from the both heating and cooling. The experimental results show that during thermal cycling up to 47 times the stress relaxation proceeds through the plastic deformation and matrix recovery.

C. Badini et al. [23] studied the thermal fatigue behaviour of a 2014/Al_2O_3-SiO_2 (Saffil® fibers) composite processed by squeeze casting. Thermal fatigue behaviour of a 2014/Saffil composite has been investigated. This composite was produced by infiltration of preforms of Saffil fibers (Al_2O_3-SiO_2 fibers) with a 2014 aluminium alloy (Al-4.7Cu-1.0Si-0.6 Mg). Thermal cycling tests were performed on specimens (either as fabricated or in the T6 temper) in the temperature range between 25 and 220°C. After 1000 cycles both the microstructure and the mechanical characteristics of the composite samples were investigated.

Pickard, S.M et al. [24] studied the behaviour of metal matrix composites during temperature cycling. Commercial purity aluminium reinforced with SiC particles has been used to model the behaviour of metal matix composites (MMCs) during thermal cycling. Above critical temperature amplitude of about 150 degC an acceleration in creep under the load occurs. This is accompanied by a reduction in the creep stress exponent from 15 to 1. The reduced stress exponent leads to a superplastic deformation behaviour with extensions in excess of 150 % recorded. Transmission electron microscopy studies of the deformed microstructures show an essentially constant dislocation structure between as-received MMCs and those after 90% strain.

P. H. Shipway, A. R. Kennedy and A. J. Wilkes[25] has studied that TiC-reinforced MMCs have been produced in a range of aluminium alloys using a novel casting technique which results in spontaneous incorporation of the particles into the melt and thus strong bonding between the particles and the matrix. The sliding wear behaviour of the extruded composites has been studied as a function of load and particle volume fraction and has been compared with a commercially available SiC-reinforced composite. In all cases, alloy reinforcement resulted in a reduction in wear rate and an increase in the load at which the transition from low rate wear to high rate wear occurred. In the low rate wear regime, the wear coefficients of all the alloys in both the reinforced and unreinforced states were similar, and since the TiC-reinforced A356 alloy was the hardest (due in part to the grain refining action of TiC), it exhibited the lowest wear rate (lower than that of the SiC-reinforced composite). Wear of the steel counterface

depended on the mechanism of wear of the composite. An increase in load generally resulted in an increase in wear rate of both the composite pin and counterface, and the reasons for this are presented. Increasing the volume fraction of particles in a composite reduces its wear rate but generally increases the wear rate of the counterface. It is suggested that when both counterface and composite wear are considered, an optimum volume fraction of particles exists at which wear is lowest.

B.N.Pramila Bai, B.S. Ramasesh and M.K. Surappa[26] presented the theory that Aluminium alloy (A356)-SiC composites containing 15 and 25 wt.% silicon carbide particles (average size 43 μm) were tested for sliding wear at different loads using a pin on disc machine. Composites exhibited better wear resistance compared with unreinforced alloy up to a pressure of 26 MPa. Scanning electron microscopy examination of worn surfaces and sub surfaces show that the presence of dispersed SiC particles help in reducing the propensity of material flow at the surface, at the same time leading to the formation of an iron-rich layer on the surface.Transition wear behaviour of SiC-particulate- and SiC-whisker-reinforced 7091 Al metal matrix composites

A. Wang and H.J. Rack[27] studied the wear behaviour of unreinforced and reinforced 7091 Al, the latter containing either 20 vol.% SiC particulates (SiC_p) or 20 vol.% SiC whiskers (SiC_w), was studied as a function of sliding distance and sliding velocity under unlubricated conditions. At sliding velocities below 1.2 m s^{-1}, SiC reinforcement does not affect wear resistance. Wear debris produced from both the unreinforced and reinforced materials was predominantly metallic and was small in dimension and dark in color. The mechanism of wear under these conditions was surface-fatigue-related surface cracking. At sliding velocities greater than 1.2 m s^{-1}, the wear rates of the reinforced materials were lower than for the unreinforced matrix. Both the unreinforced alloy and the SiC-reinforced composites exhibited elevated wear rates during the initial period of sliding, the mechanism of wear under these conditions, *i.e* high velocity and short sliding distance, being controlled by subsurface-cracking-assisted adhesive transfer and by abrasion. During steady state sliding, these elevated wear rates were maintained by the unreinforced alloy, reduced wear rates being observed in the reinforced composites. The initial wear rates of the composites depend strongly upon reinforcement orientation, the highest wear rates being observed the perpendicularly oriented SiC_w composite. However, the steady state wear rates of the composites were generally independent of reinforcement geometry (particulate *vs.* whiskers) and orientation (perpendicular *vs.* parallel) with the exception of wear at 3.6 m s^{-1} where the parallel-oriented SiC_w composite was superior

S. Wilson and A. T. Alpas [28] studied the Effect of temperature on the sliding wear performance of Al alloys and Al matrix composites. The effect of ceramic particulate and graphite additions on the high temperature dry sliding wear resistance of two Al alloys was studied. The experiments were performed using a ring-on-flat sliding contact configuration against hardened SAE 52100 bearing steel counterfaces on an apparatus built for testing at controlled temperatures. Conditions were selected such that the materials in contact were kept in an isothermal atmosphere and the generation of frictional heat was minimised by the use of a low load (11.55 N) and sliding speed (0.1 m s^{-1}). For unreinforced 6061 Al and A356 Al alloys a transition from mild to severe wear occurred in the ranges 175–190 °C and 225–230 °C respectively. With the addition of 20 vol.% Al_2O_3 to 6061 Al, the mild to severe wear transition was raised to a range between 310–350 °C. Likewise, an addition of 20 vol.% SiC to the A356 Al increased this transition to 440–450 °C. A hybrid A356 Al composite containing 20 vol. % SiC and 10 vol. %

graphite remained in a mild wear regime at the highest test temperature of 460 °C. All the reinforced alloys were able to withstand considerable thermal softening effects while remaining in a mild sliding wear regime. This is attributable to the formation of protective transfer layers of comminuted reinforcing particulates and transferred steel debris from slider counterfaces. Graphite in the hybrid composite introduced greater mild wear losses compared with the other composites due to increased friability and contact surface extrusion effects. The absence of severe wear phenomena in this composite contributes to the inhibition of comminution and fracture by graphite entrained in the surface tribolayer.

F. M. Hosking, F. Folgar Portillz, R. Wunderlin and R. Mehrabian [29] studied Composites of aluminium alloys. fabrication and wear behaviour. processes for fabrication of aluminium-alloy composites containing paniculate non-metals, the net shape forming of these composites, their microstructures, their friction and wear behaviours and their mechanical properties are described. Composites of two wrought (2014 and 2024) and one cast (201) aluminium alloys containing 2 to 30 wt% of Al_2O_3 and SiC particles in the size range of 1 to 142 μm were prepared. The non-metallic particles were added to a partially-solid vigorously-agitated matrix alloy. The particles were then retained in the matrix until interface interaction, for example, the formation of $MgAl_2O_4$ spinel in the case of Al_2O_3 particles, were faciliated. These composites were solidified and subsequently reheated to above their liquidus temperature and formed under high pressure in a closed-die forging type of apparatus. Composites with particulate additions of size larger than 5 μm possessed homogeneous structures; particles of size 1 μm, however, tended to cluster. The wear behaviour of the composites was studied using a pin-on-disc type machine. It was shown that composites containing large amounts of non-metals, $\approx$20 wt%, exhibit excellent wear resistance whilst those with small to moderate amounts of non-metals possess tensile properties comparable to the matrix alloy. Increasing the amount of particulate additions results in reduced ductility. Finally, a method was investigated of producing components with high weight-fractions of non-metals near their surface

In past, significant work has been done on production and characterization of MMC's using different methods. A number of researchers have done experimental analysis on composites subjected to thermal cycling, but the effects of thermal cycling on Aluminium composites using SiC and Fly ash together have not been investigated. The present work will focus on fabrication and characterization of Al matrix composite reinforced with varying quantities of SiC and Flyash.

CHAPTER 3 PROBLEM FORMULATION

In present work, the Effects of Thermal Cycling on Cast Al-SiC-fly ash Composites are investigated. Metal matrix composites (MMCs) are a range of advanced materials that can be used for a wide range of applications within the aerospace, automotive, nuclear, biotechnology, electronic and sporting goods industries and are rapidly becoming candidates as structural materials for high temperature applications. There has been an increasing interest in composites containing low density and low cost reinforcements. Among various discontinuous reinforcements used, fly ash is one of the most inexpensive and low density reinforcement available in large quantities as solid waste by-product during combustion of coal in thermal power plants. Hence, composites with fly ash as reinforcement are likely to overcome the cost barrier for wide spread applications in automotive and small engine applications.

Material selected for experimental Purposes was Al/SiC 15p.The addition of Fly Ash is done to it in 5 %, 10 % and 15 % by weight reducing the SiC proportion. The specimens produced are tested and then subjected to varying temperatures (400^0C to 450 ^{0}C). Once again different tests are performed on specimens after thermal cycling to find change in properties of material.

3.1 Objective of Work

To see effect of thermal cycles on specimens, which are prepared by varying the fly ash content in original material. In initial stage the specimen are produced using stir casting technique. Different tests are performed on these test samples. The specimens are then subjected to varying temperature 100 °C to 450°C and changes in the properties of the specimens are observed.

The tests performed on the samples are as below:

1. Micro Hardness Test
2. The Microstructure (SEM)
3. X-Ray Diffraction Test
4. Wear Test

3.2. Work Plan for Experiments

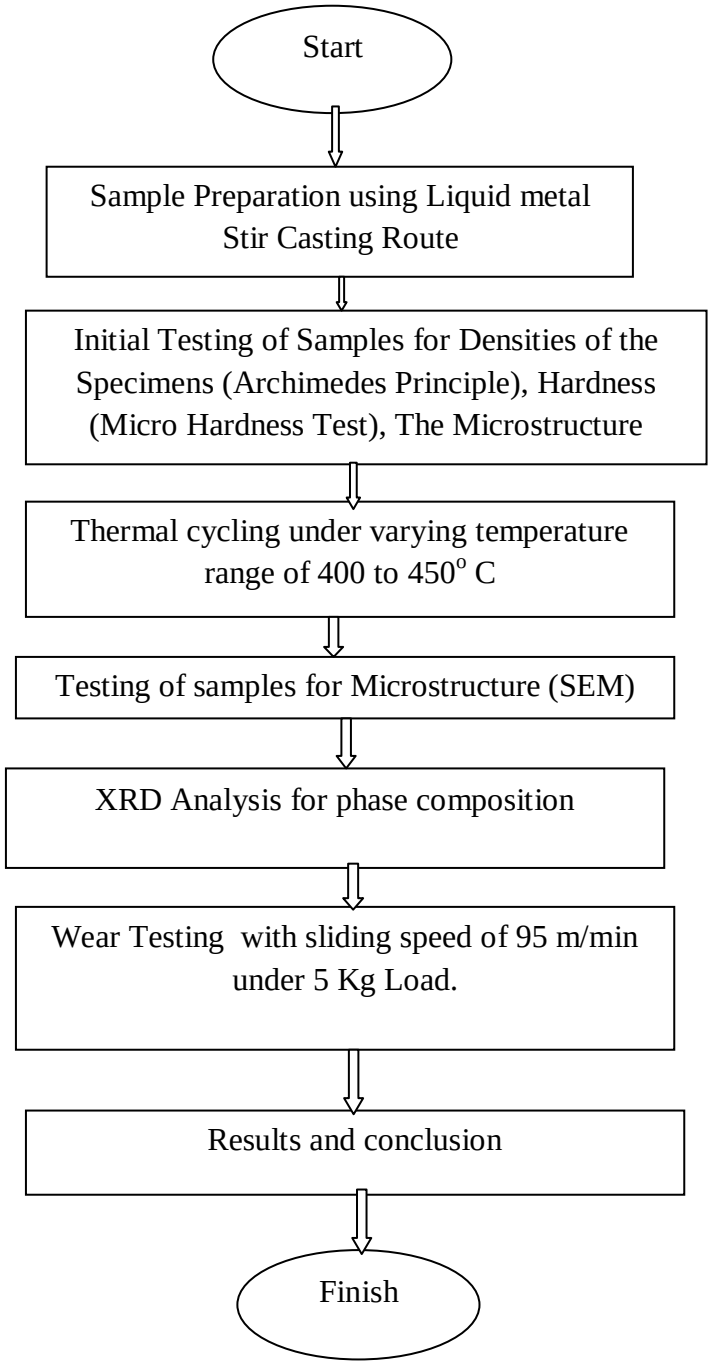

Figure 3.1.- Work Plan for Experiments

CHAPTER 4 EXPERIMENTAL WORK

4.1. Experimental Setup

For performing the stir casting operation and testing of composites the following machines/equipments were used:

1. A resistance heated muffle furnace
2. Radial drilling machine
3. Graphite crucible
4. Vicker's Micro Hardness Testing Machine
5. Graphite stirrer
6. Stainless steel rod (SS304l) of diameter 12mm, Length 500mm
7. C-clamp
8. Disc type wear testing machine
9. Vernier calliper
10. Scanning electron microscope
11. Multifunction Infrared Thermometer

4.2 Preparation of Samples

Pure Aluminium was melted in a crucible by heating it in a resistance furnace set at 1100°C for three to four hours. Hardness of Pure Aluminium on Rockwell Hardness testing machine was 49 HRB. The silicon carbide particles and as received dry fly ash from Bathinda thermal plant were preheated at 1100^{o}C and 200^{o}C respectively for one to three hours to make their surfaces oxidised. The furnace temperature was first raised above the liquidus temperature of Aluminium near about 750^{o}C to melt the Al completely and was then cooled down just below the liquidus to keep the slurry in Semi solid state. Automatic stirring was carried out with the help of radial drilling machine for about 20 minutes at stirring rate of 290 RPM. At this stage, the preheated SiC particles and dry fly ash particles were added manually to the vortex. In the final mixing processes the furnace temperature was controlled within 700 ± 10^{o}C. The mixture was allowed to cool down in the crucible for few hours.

The SiC particles and dry fly ash particles were observed to be accommodated on the boundaries. The presence of reinforcement throughout the specimen was inspected by cutting the casting at different locations and under microscopic examination. Taking the same route four specimens with different compositions of SiC and Flyash were cast.

Table 4.1. - Composition of Samples

Composition				
Sample No.	**Aluminium(gm)**	**SiC(gm)**	**Fly Ash(gm)**	**Remarks**
1	746	132	0	Weight of sample=878 gm
2	746	88	43	SiC=10%, Fly Ash=5%
3	746	43	88	SiC=5%, fly Ash=10%
4	746	0	132	Fly Ash=15%

Figure 4.1.- Preparation of Samples in Electrical Resistance furnace

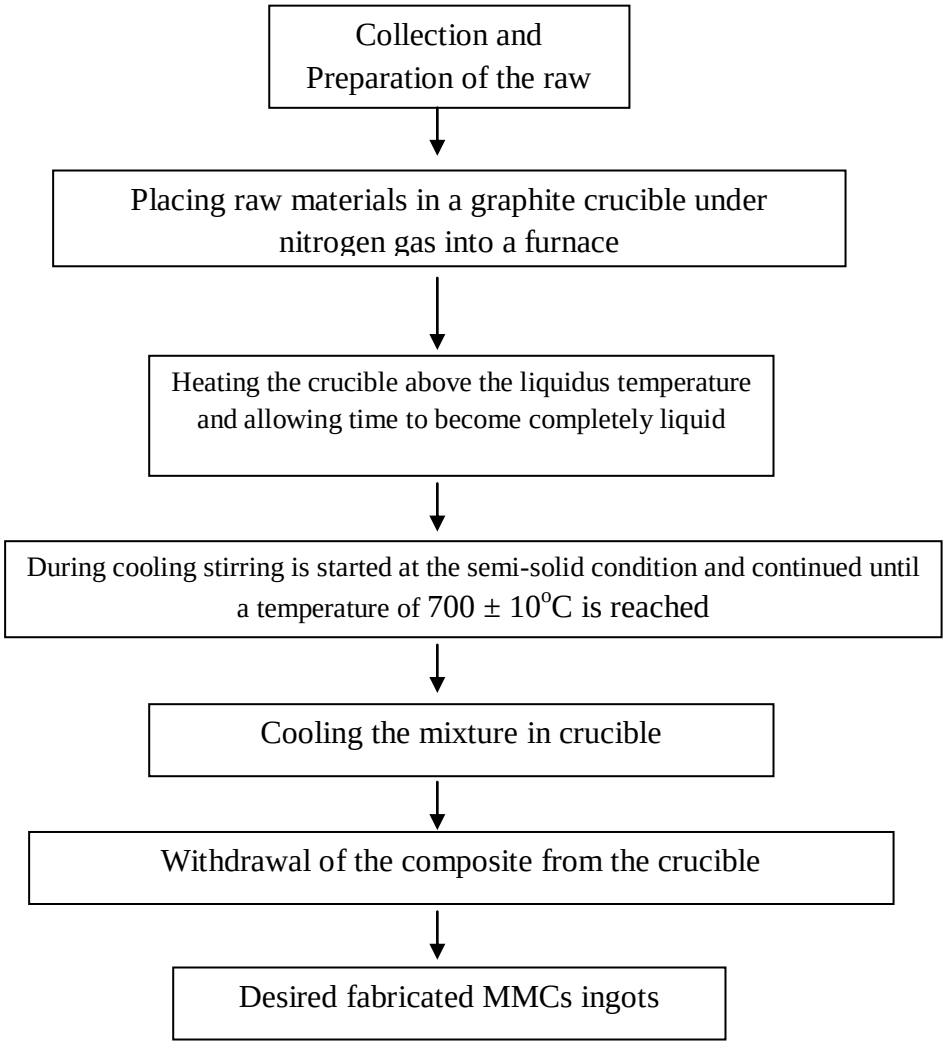

Figure 4.2. - Flow Chart Showing Steps in involved in Stir Casting

4.3 Experimental Procedure

Following procedure was followed after the casting operation

1. Specimens, prismatic in shape with dimensions 45 mm x 20 mm and 23 mm (L x b x t) were cut from the cast composite.
2. The SEM and XRD analysis was done for the samples.
3. Micro hardness of specimen was measured.
4. Each specimen was subjected to a compressive load of 74.9 N.
5. The specimens were then heated in the furnace to a temperature range of 400 – 450 ^{0}C.
6. Air cooling of specimens was then done under forced convection so to lower the specimen temperature to room temperature.
7. Each specimen was subjected to five such thermal cycles.
8. To check the dimensional stability, the change in dimensions of each specimen was noted.
9. Step 2 and 3 were repeated.
10. To carry out the wear tests on pieces of size 15 mm square were cut.
11. Pins of dimensions of 8 mm diameter and 50 mm length were prepared.
12. Wear test was performed on each specimen at 5Kg load and 300 rpm for 30 minutes.
13. The data related to wear test was recorded for each specimen before and after thermal cycling.

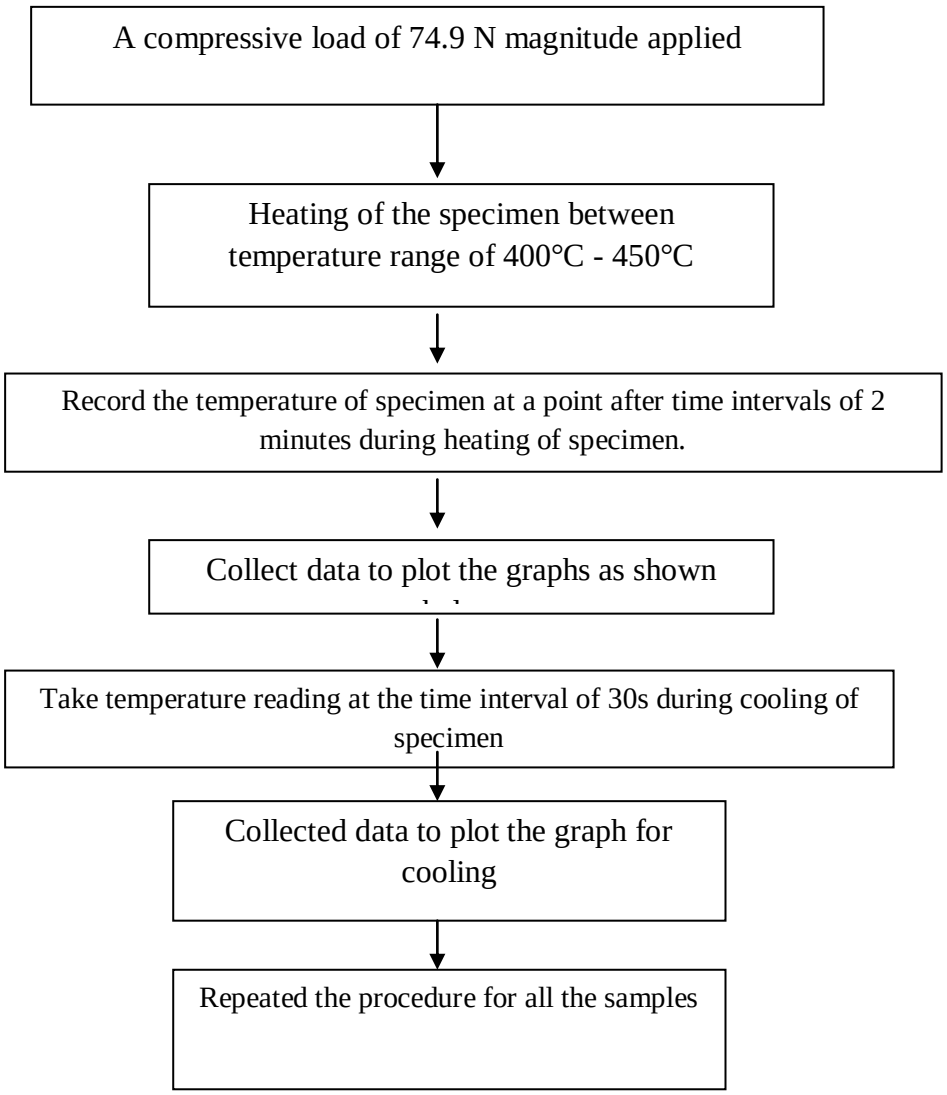

Figure 4.3.- Flow Chart showing thermal cycling of Samples

CHAPTER 5 TESTING RESULTS AND DISCUSSIONS

5.1 visual observations

After the thermal cycling of specimens under the same compressive load, the deformations of different specimens were found to be different. The change of dimensions, which can be considered as a measure of structural stability under thermal cycling, is given in table

Table 5.1- Changes after thermal expansion

Sample No.	Before thermal expansion			After thermal Expansion		
	Length (mm)	Width (mm)	Thickness (mm)	Length (mm)	Width (mm)	Thickness (mm)
1	45	20	23	43	20.8	23.5
2	45	20	23	44	18	21
3	45	20	23	44	21.18	24
4	45	20	23	45	20.05	23

A comparison of change in dimensions of all specimen after thermal cycling shows that the deformation of specimen no. 4 is minimum. Therefore addition of flyash upto 15% by weight improved the dimensional stability of specimen.

5.1.1 Pictorial comparison of Samples Before and After Thermal Cycling

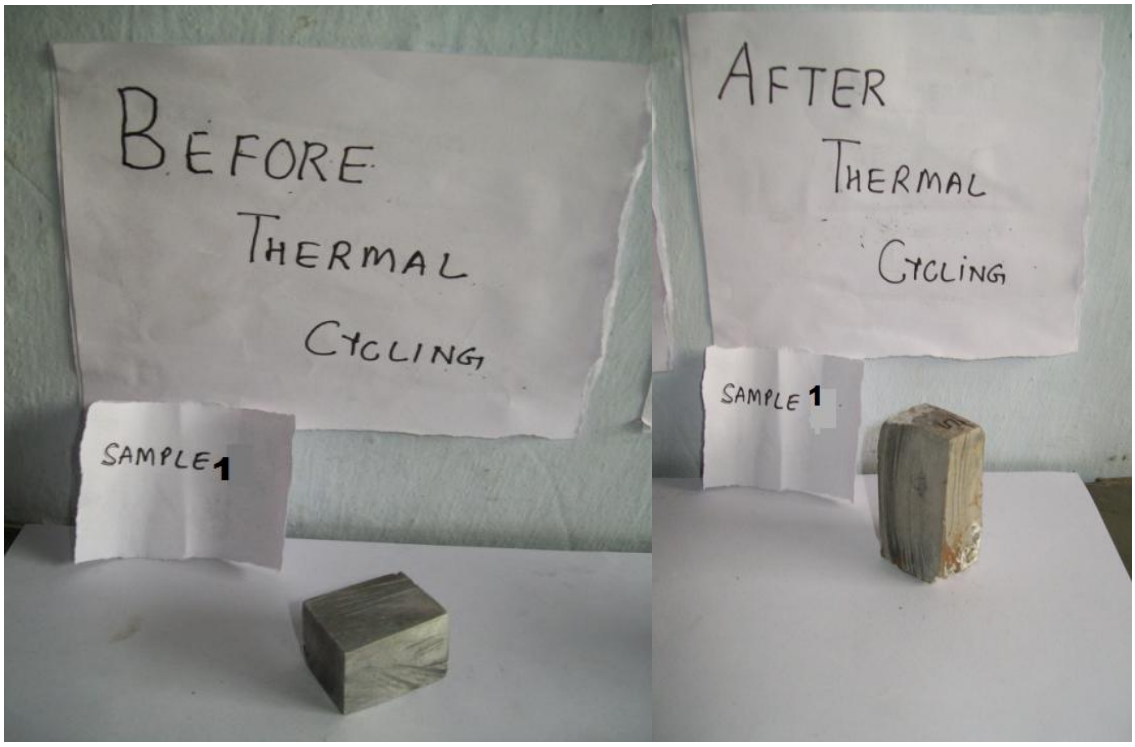

Fig 5.1- Pictures of Sample no.1 before and after Thermal Expansion

Fig 5.2- Pictures of Sample no.2 before and after Thermal Expansion

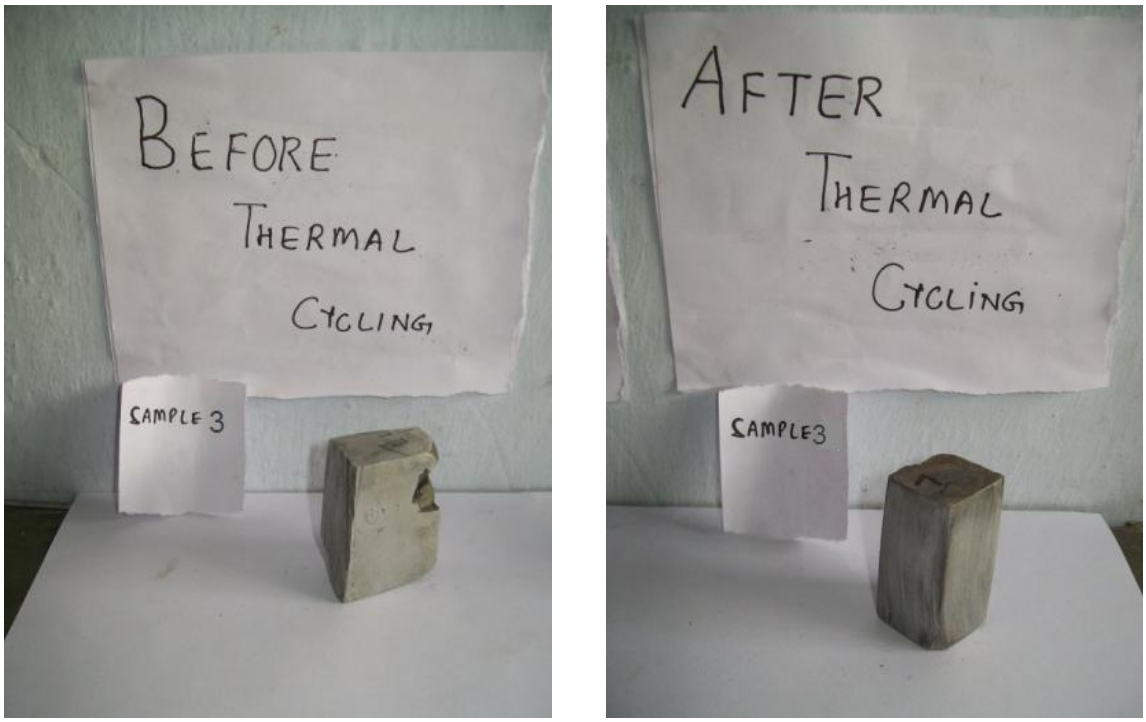

Fig 5.3- Pictures of Sample no.3 before and after Thermal cycling

Fig 5.4- Picture of Sample 4 after Thermal cycling

5.1.2 Temperature- Time plots

During thermal cycling the samples were subjected to temperature range of 400 – 450 ^{0}C and then cooled to room temperature. The temperature of specimen was measured after every 2 minutes during heating and after every 30 s during cooling. As experimentally found, the thermal conductivity of dry flyash is less than of SiC, therefore addition of flyash in higher proportion in Al-SiC reduces the rate of heating and cooling. The following graphs were then plotted to investigate the effect of addition of flyash to Al-SiC mixture.

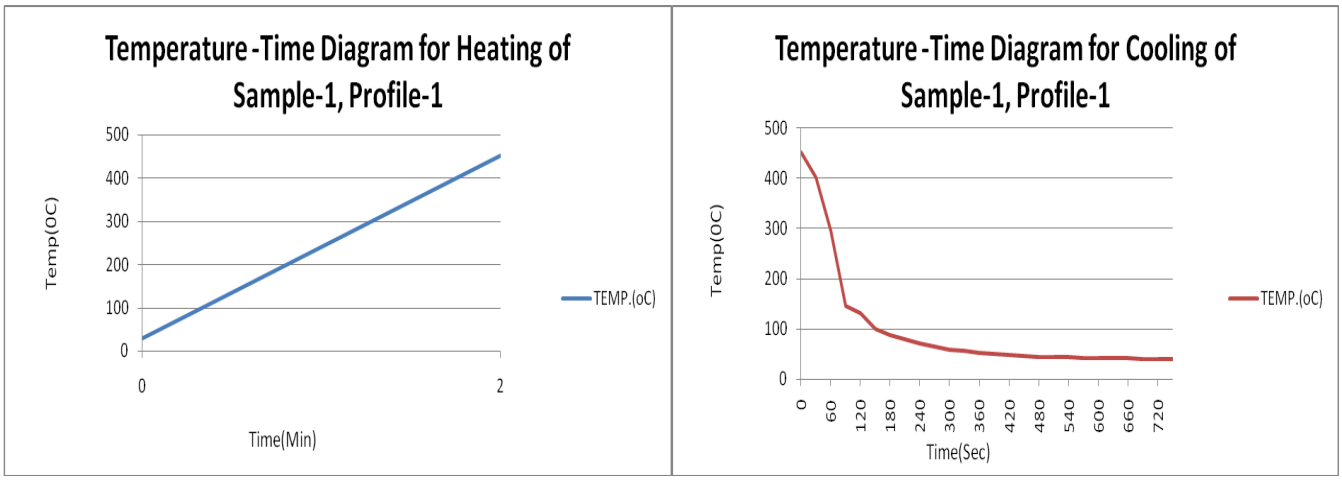

Figure 5.5.- Temperature -Time Plot for Heating and cooling of Sample-1, Profile-1

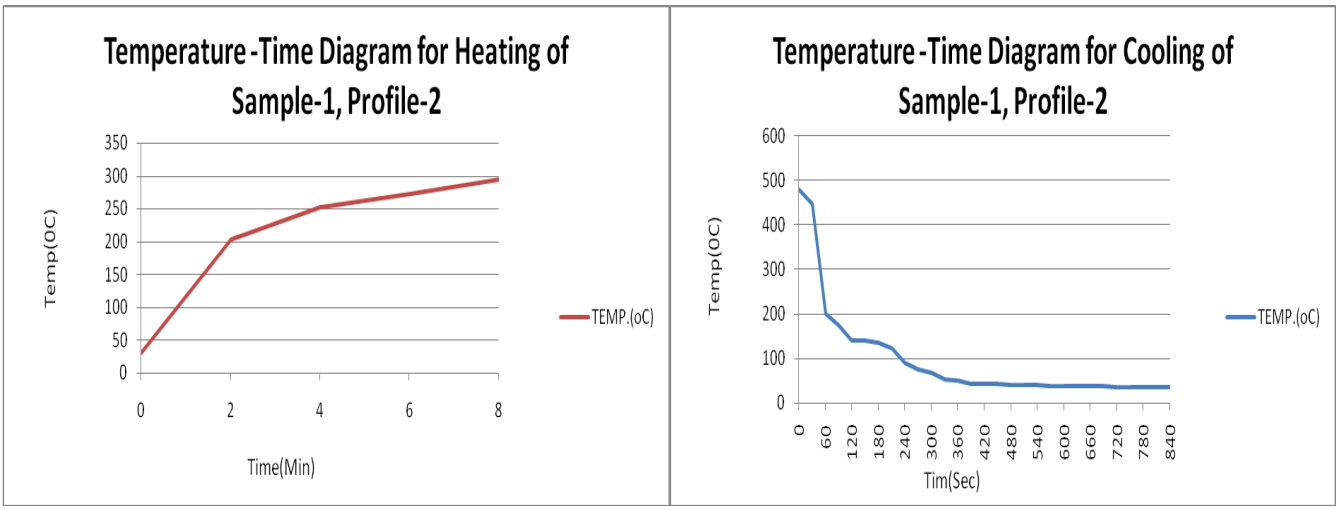

Figure 5.6.- Temperature -Time Plot for Heating and Cooling of Sample-1, Profile-2

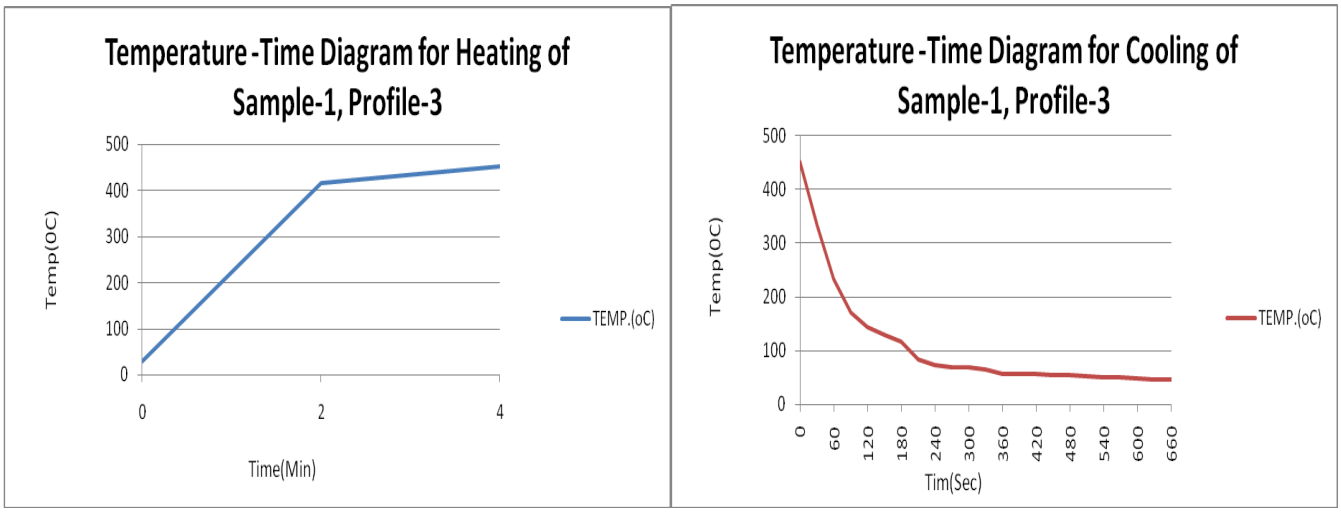

Figure 5.7.- Temperature -Time Plot for Heating and Cooling of Sample-1, Profile-3

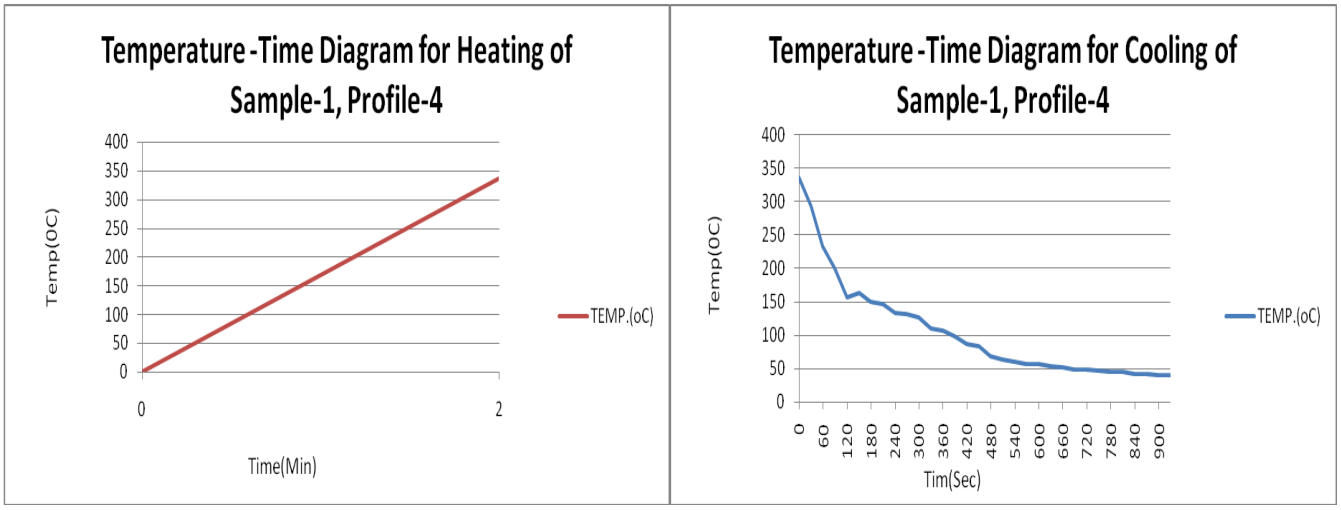

Figure 5.8.- Temperature -Time Plot for Heating and cooling of Sample-1, Profile-4

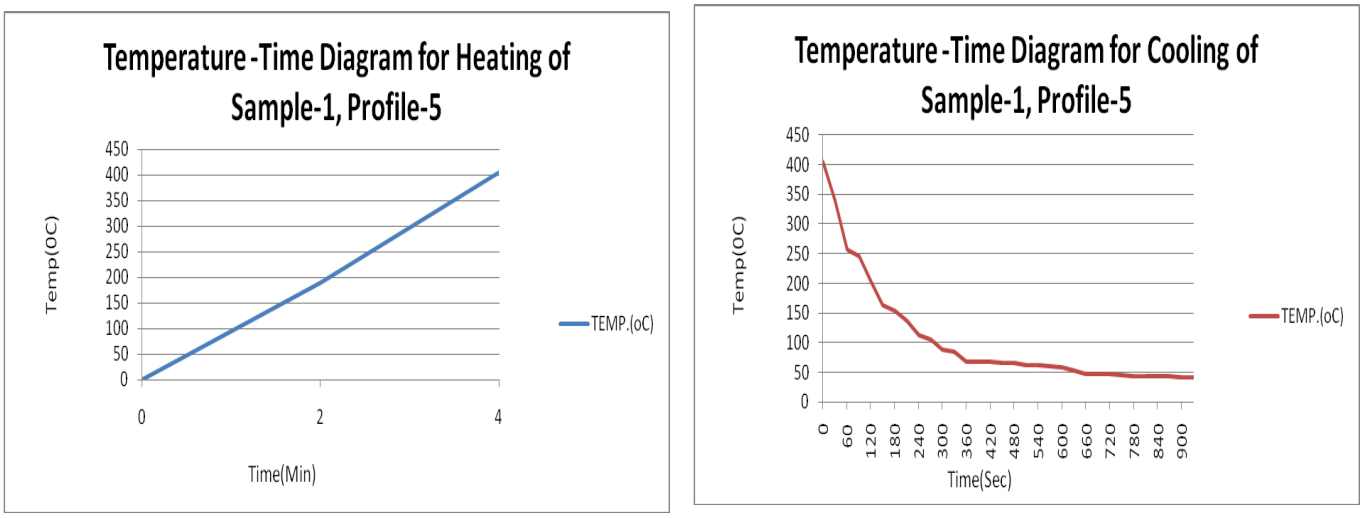

Figure 5.9-Temperature –Time Plot for Heating and cooling of Sample-1 Profile-5

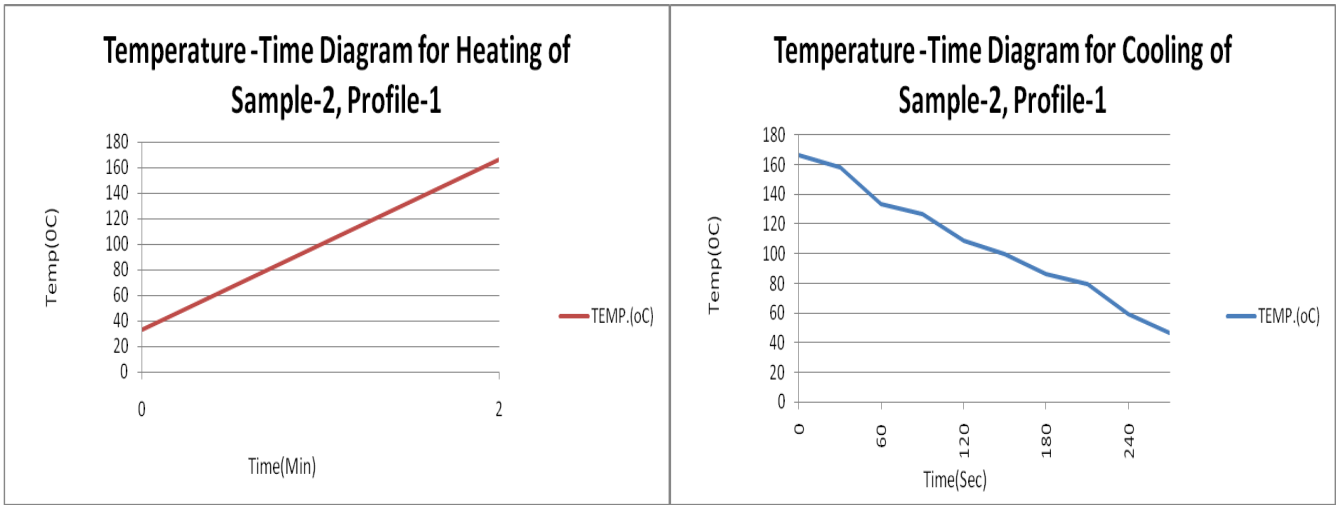

Figure 5.10.- Temperature -Time Plot for Heating and cooling of Sample-2, Profile-1

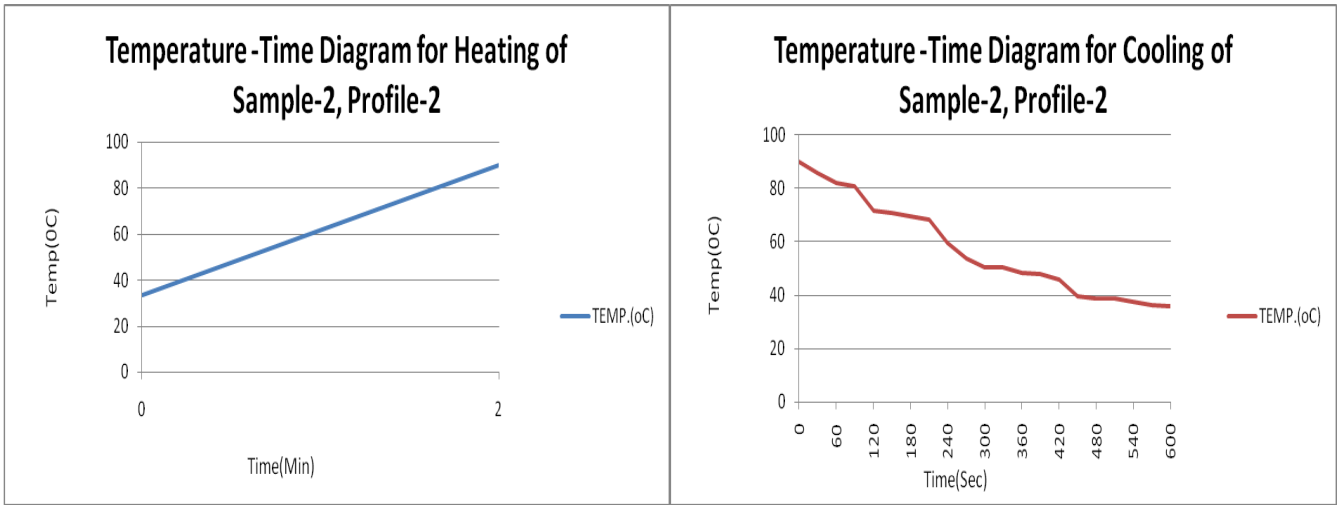

Figure 5.11.- Temperature -Time Plot for Heating and cooling of Sample-2, Profile-2

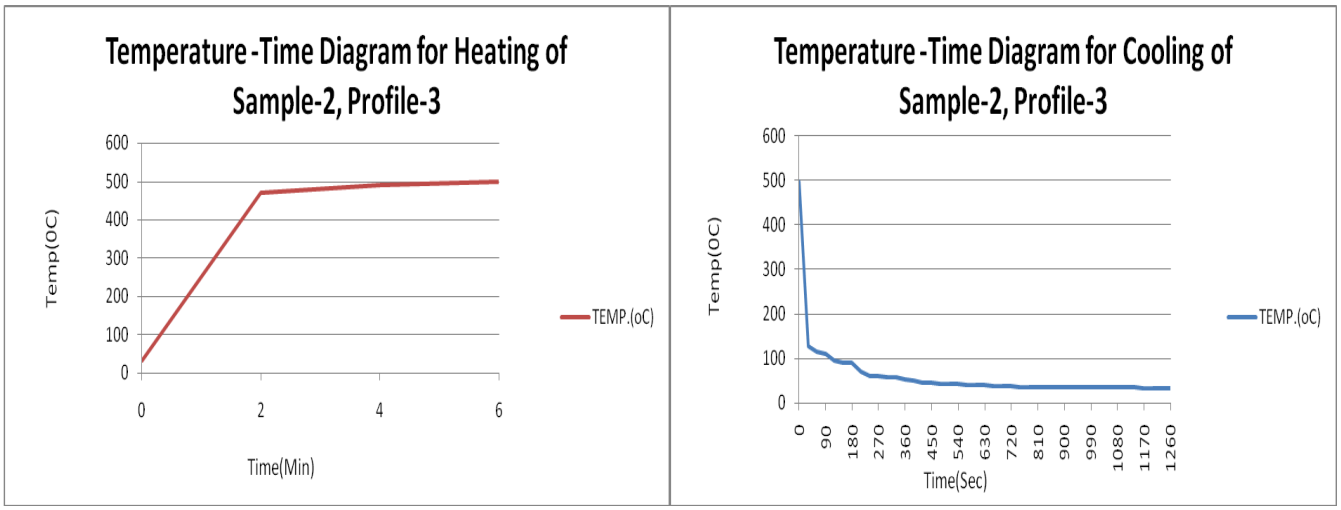

Figure 5.12.- Temperature -Time Plot for Heating and cooling of Sample-2, Profile-3

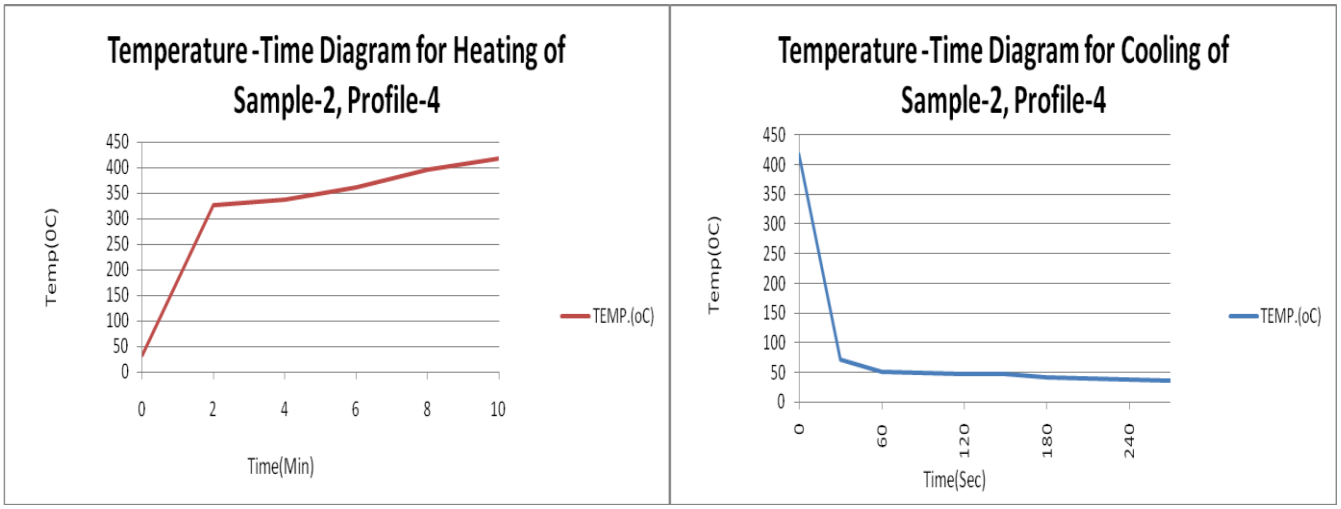

Figure 5.13.- Temperature -Time Plot for Heating and cooling of Sample-2, Profile-4

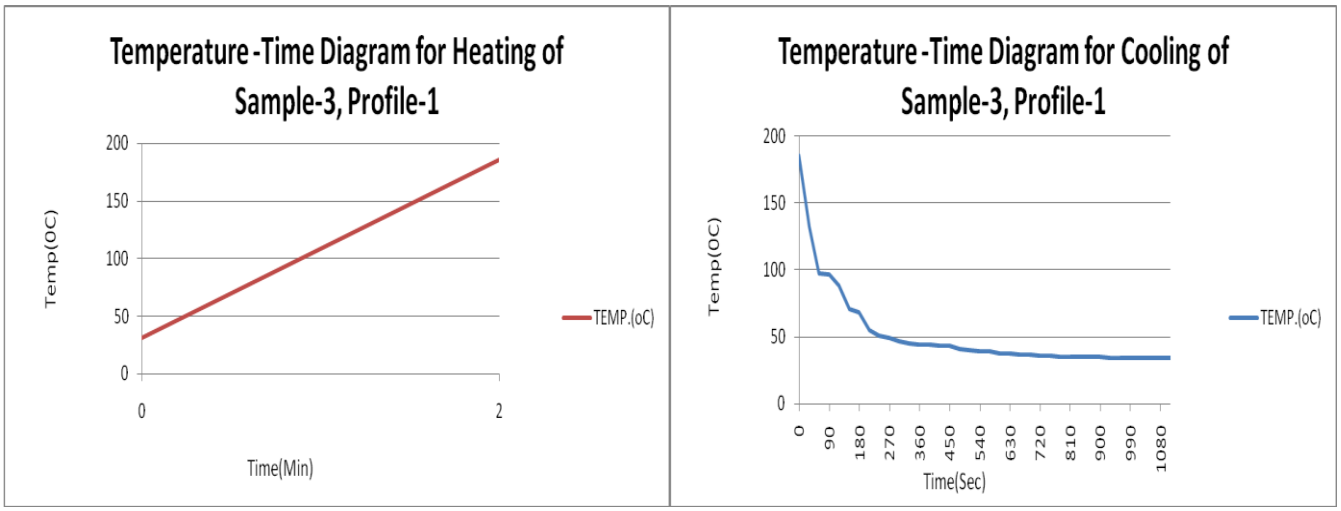

Figure 5.14.- Temperature -Time Plot for Heating and cooling of Sample-3, Profile-1

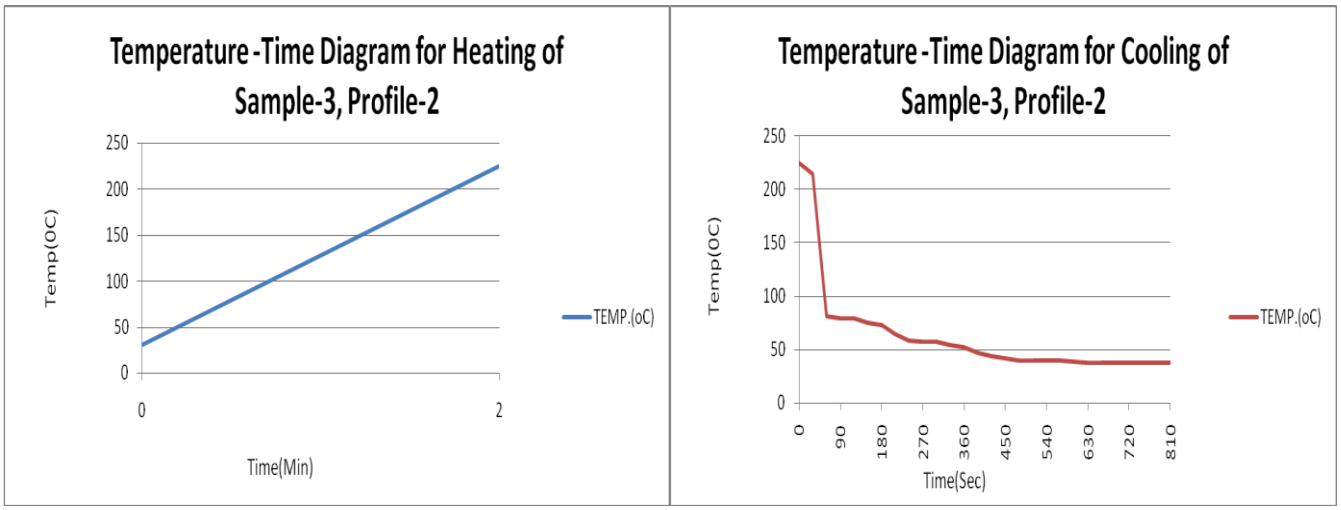

Figure 5.15.- Temperature -Time Plot for Heating and cooling of Sample-3, Profile-2

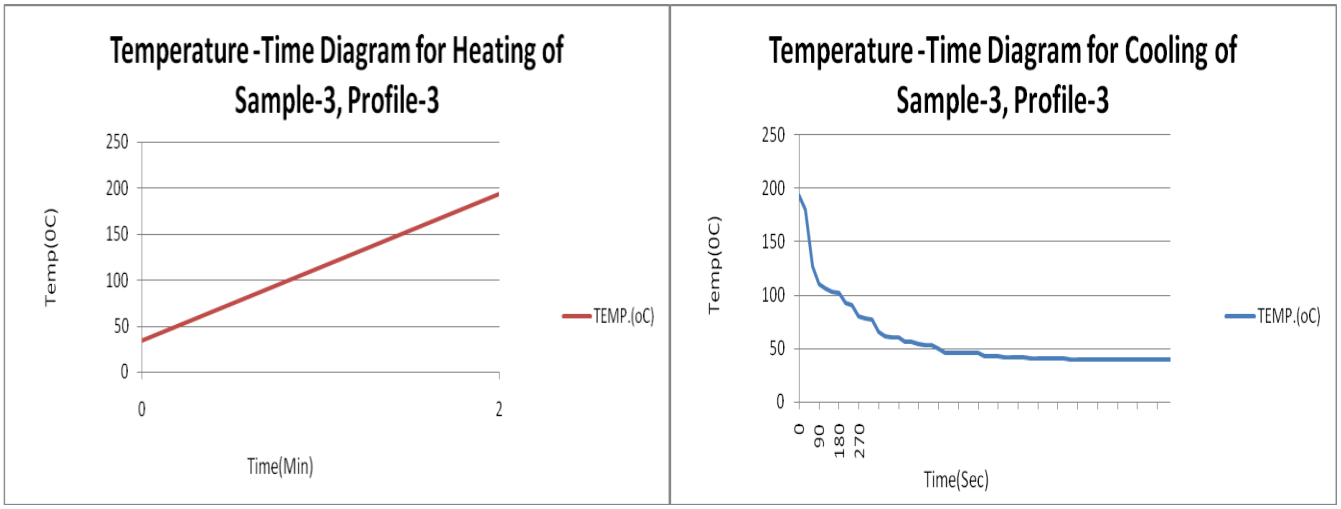

Figure 5.16.- Temperature -Time Plot for Heating and cooling of Sample-3, Profile-3

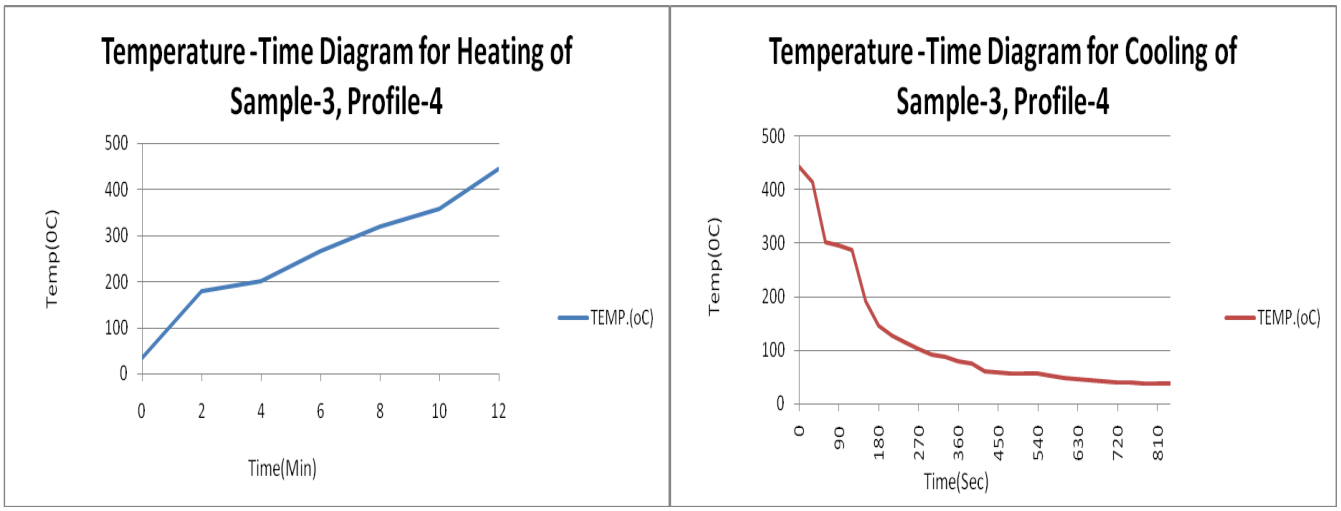

Figure 5.17.- Temperature -Time Plot for Heating and cooling of Sample-3, Profile-4

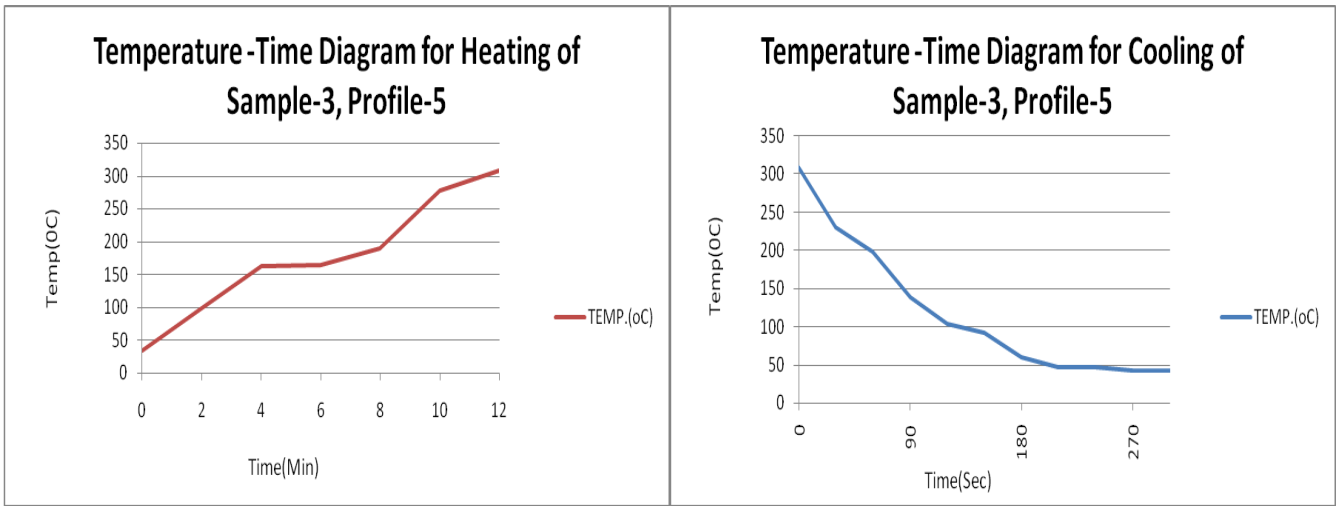

Figure 5.18.- Temperature -Time Plot for Heating and cooling of Sample-3, Profile-5

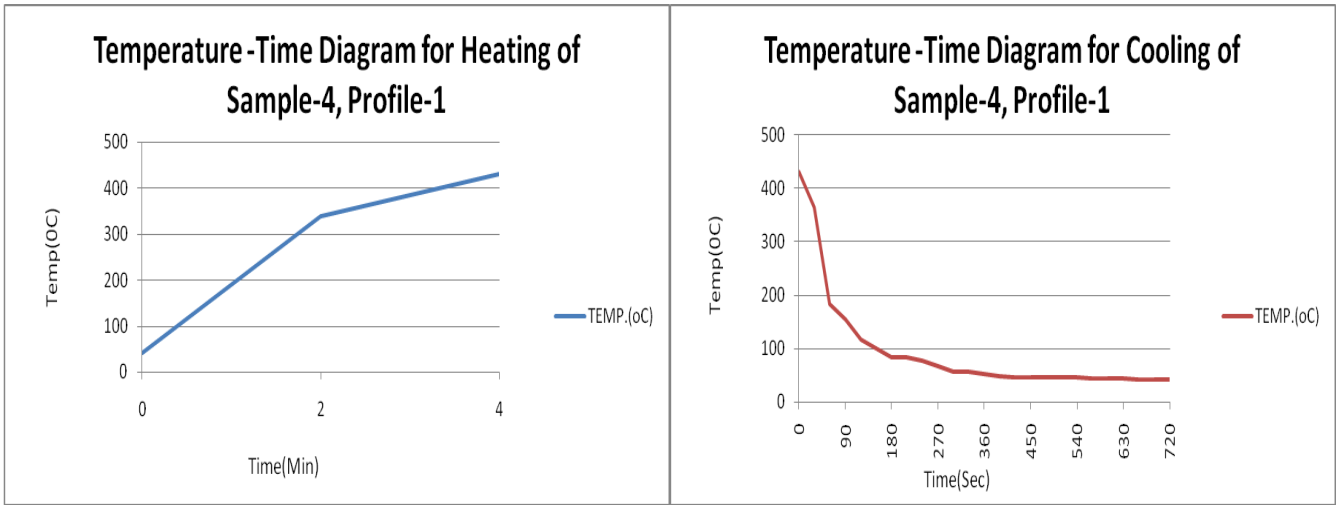

Figure 5.19- Temperature -Time Plot for Heating and cooling of Sample-4, Profile-1

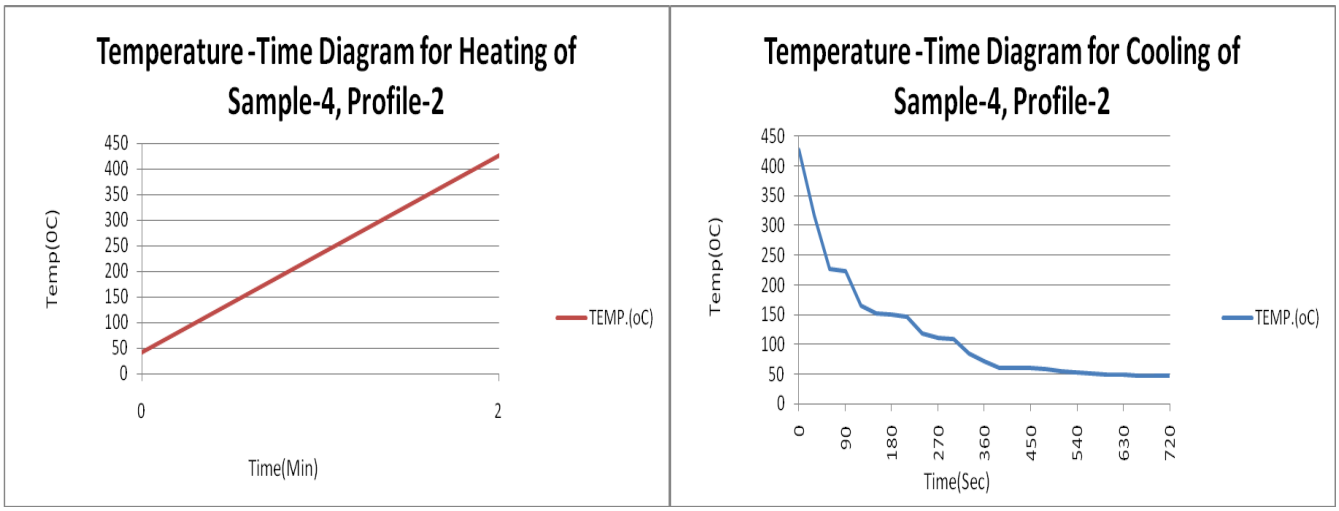

Figure 5.20.- Temperature -Time Plot for Heating and cooling of Sample-4, Profile-2

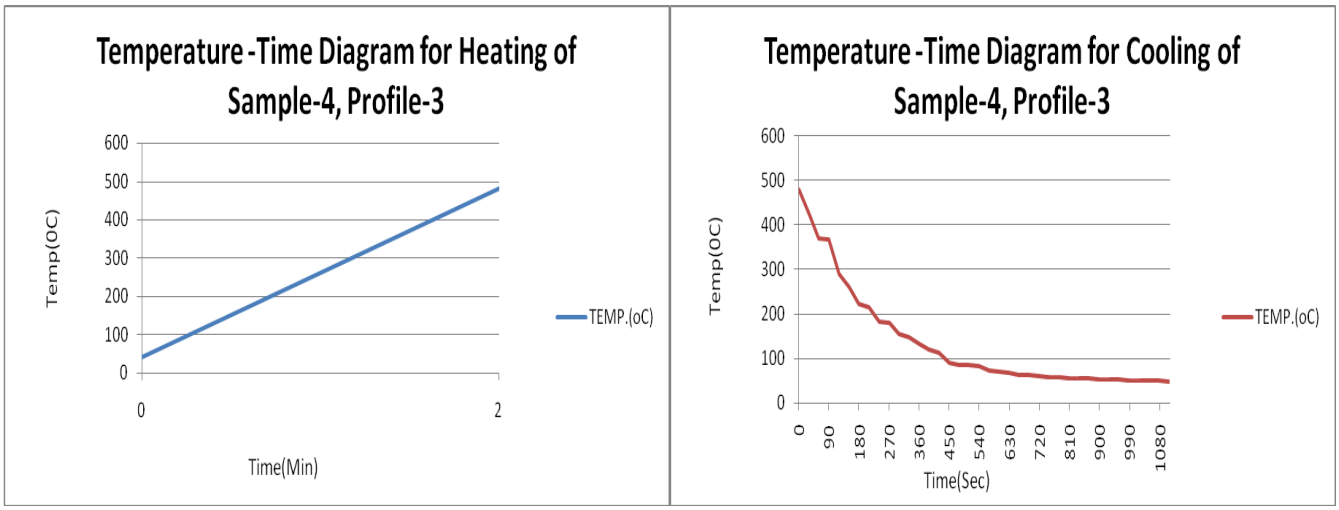

Figure 5.21.- Temperature -Time Plot for Heating and cooling of Sample-4, Profile-3

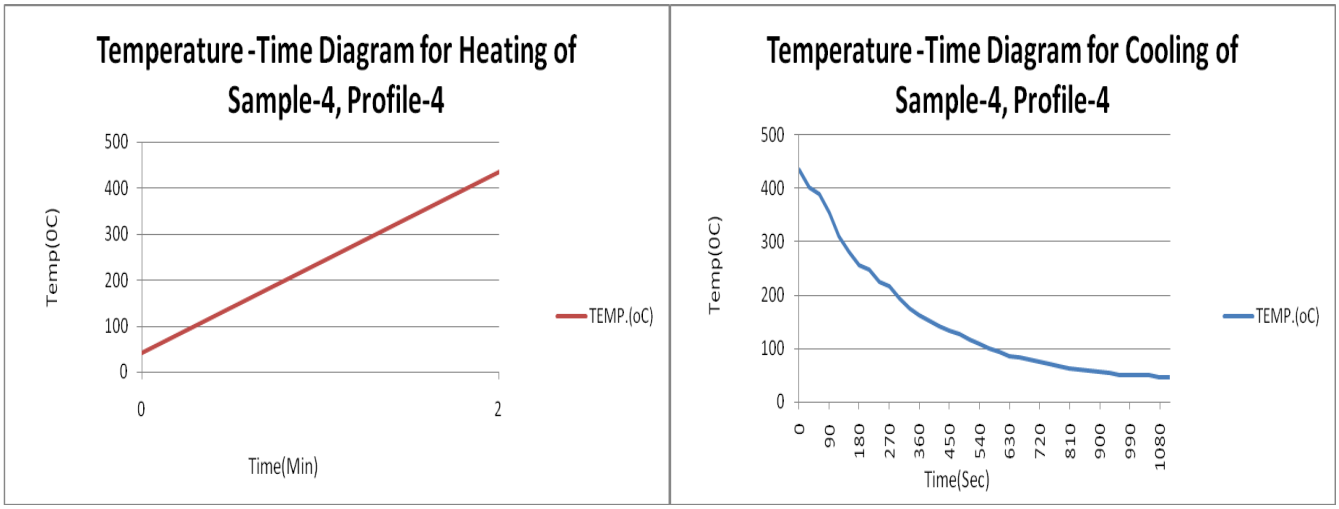

Figure 5.22.- Temperature -Time Plot for Heating and cooling of Sample-4, Profile-4

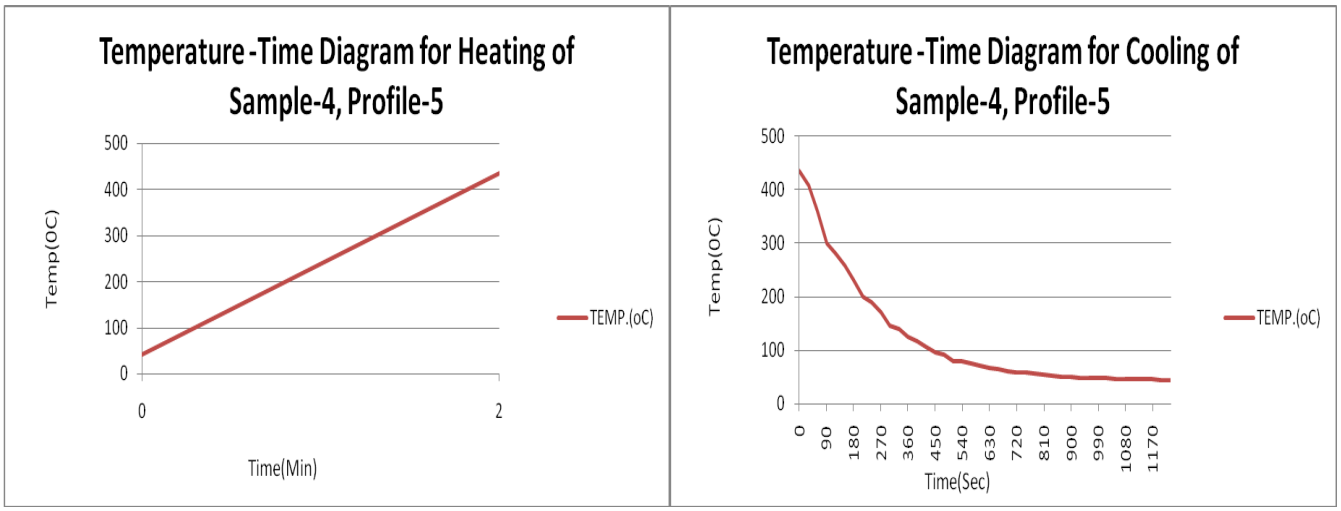

Figure 5.23.- Temperature -Time Plot for Heating and cooling of Sample-4, Profile-5

5.2 Results of XRD and SEM on Samples

XRD and SEM analysis were conducted on all the samples from 1 to 4.
In XRD, the physical content of the constituents present in the samples are indicated in the form of a graph and in SEM, images of the microstructure of the samples are taken at 100,200,500 &1000 micron. Their results have compiled and as shown below:

Figure 5.24 below shows the XRD of Sample No-1 and Table no. 5.2 shows the %age of material present in Sample No-1 before thermal cycling. Similarly Fig 5.25 shows XRD of Sample no.1 and Table 5.3 shows %age of material in the sample after thermal cycling.

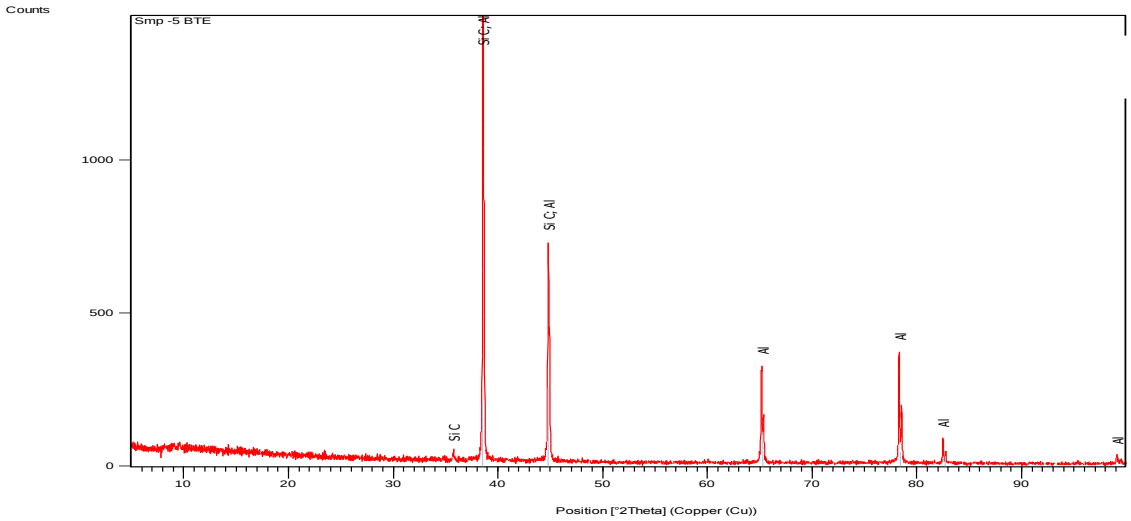

Figure 5.24.- X.R.D of Sample No.-1(Before Thermal cycling)

Table 5.2- %age of material in sample no.1 (Before thermal Cycling)

Visible	Ref. Code	Score	Compound Name	Displacement [°2Th.]	Scale Factor	Chemical Formula	SemiQuant [%]
*	01-089-3067	12	Moissanite-174R, syn	0.000	0.043	Si C	49
*	01-071-3760	22	Aluminium	0.000	0.202	Al	51

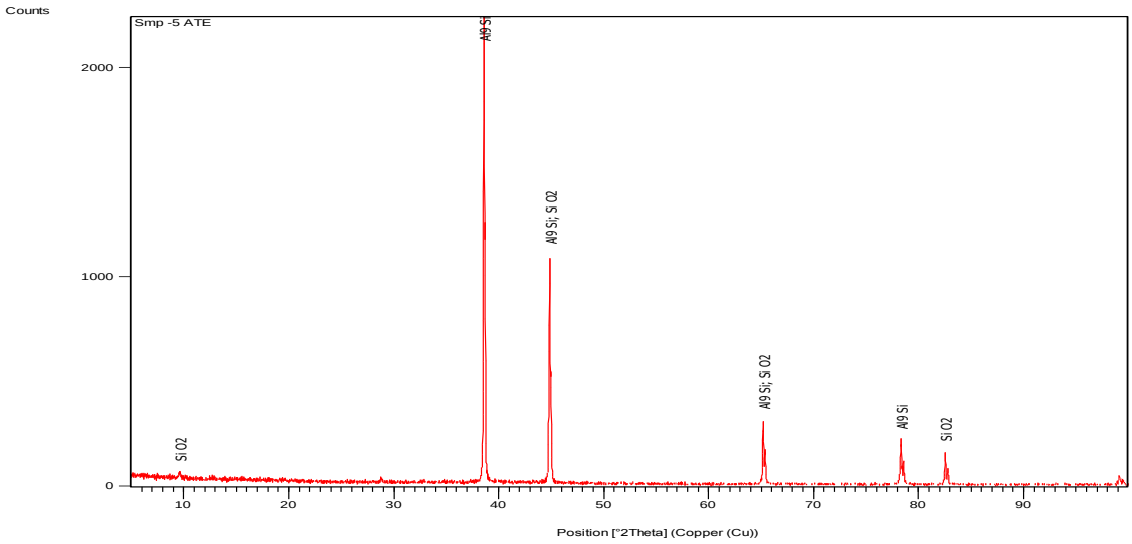

Figure 5.25.-X.R.D of Sample No.-1(After Thermal Cycling)

Table 5.3- %age of material in sample no.1 (After thermal Cycling)

Visible	Ref. Code	Score	Compound Name	Displacement [°2Th.]	Scale Factor	Chemical Formula	SemiQuant [%]
*	03-065-8554	43	Silicon Aluminum	0.000	0.797	Al9 Si	98
*	01-075-3905	16	Silicon Oxide	0.000	0.015	Si O2	2

`

Figure 5.26 Shows SEM images of sample no.2 before thermal cycling at 100,200,500 and 1000 microns in which the internal structure of the sample may be seen before Thermal cycling. Figure no. 5.27 and Table no. 5.4 shows XRD results of Sample no.2 before thermal cycling. Similarly

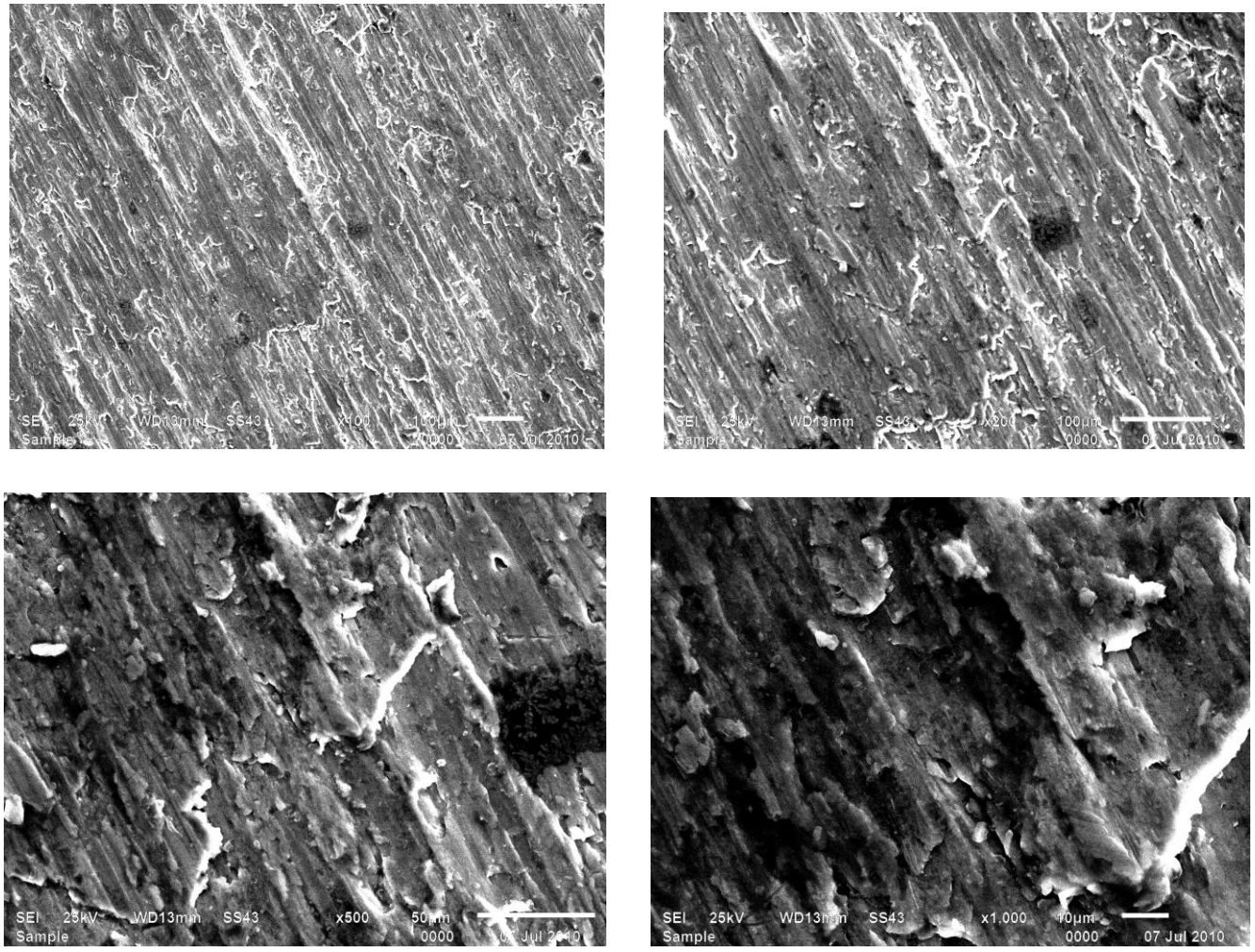

Figure 5.26. –SEM images of Sample no.2 at 100,200,500 and 1000 Microns (Before Thermal Cycling)

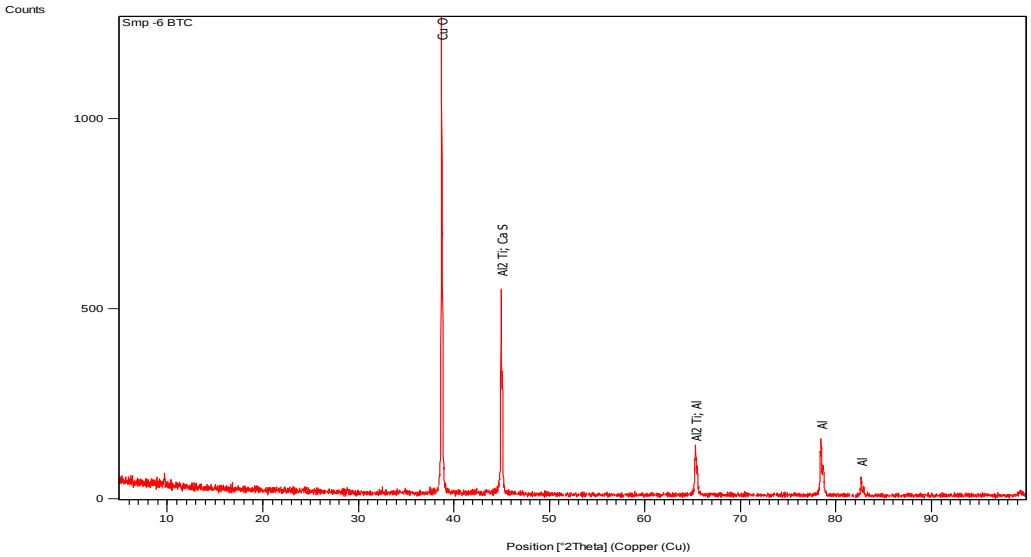

Figure 5.27. - X.R.D of Sample No.-2(Before Thermal cycling)

Table 5.4.- %age of material in Sample no.2 (Before Thermal Cycling)

Visible	Ref. Code	Score	Compound Name	Displacement [°2Th.]	Scale Factor	Chemical Formula	SemiQuant [%]
*	01-070-6831	11	Copper Oxide	0.000	0.621	Cu O	50
*	01-072-8513	20	Aluminum Titanium	0.000	0.215	Al2 Ti	14
*	03-065-0894	12	Calcium Sulfide	0.000	0.653	Ca S	32
*	01-071-4625	47	Aluminum, syn	0.000	0.055	Al	4

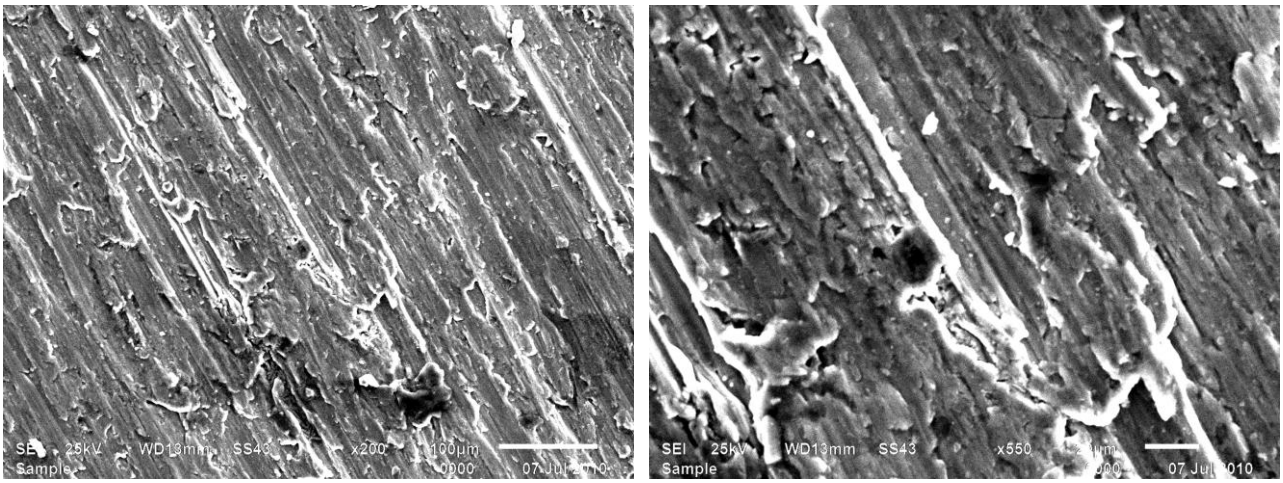

Figure 5.28- SEM images of Sample- 2(After Thermal Cycling)

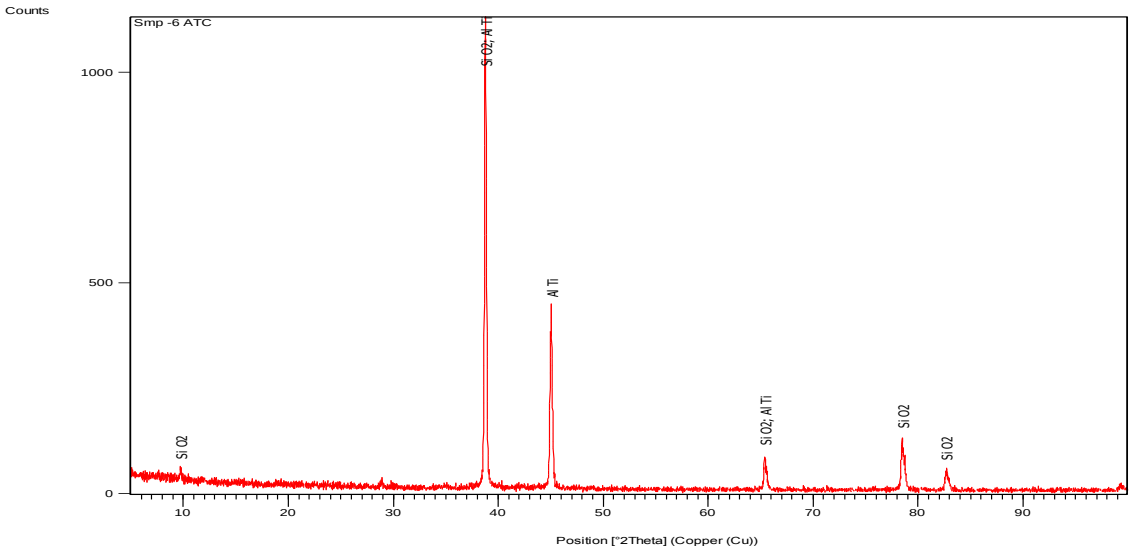

Figure 5.29- XRD graph of Sample -2 (After Thermal cycling)

`

Table 5.5- %age of material in Sample no. 2 (After Thermal Cycling)

Visible	Ref. Code	Score	Compound Name	Displacement [°2Th.]	Scale Factor	Chemical Formula	SemiQuant [%]
*	01-073-3408	22	Silicon dioxide, Zeolite	0.000	0.028	Si O2	3
*	03-065-8566	38	Aluminum Titanium	0.000	0.592	Al Ti	97

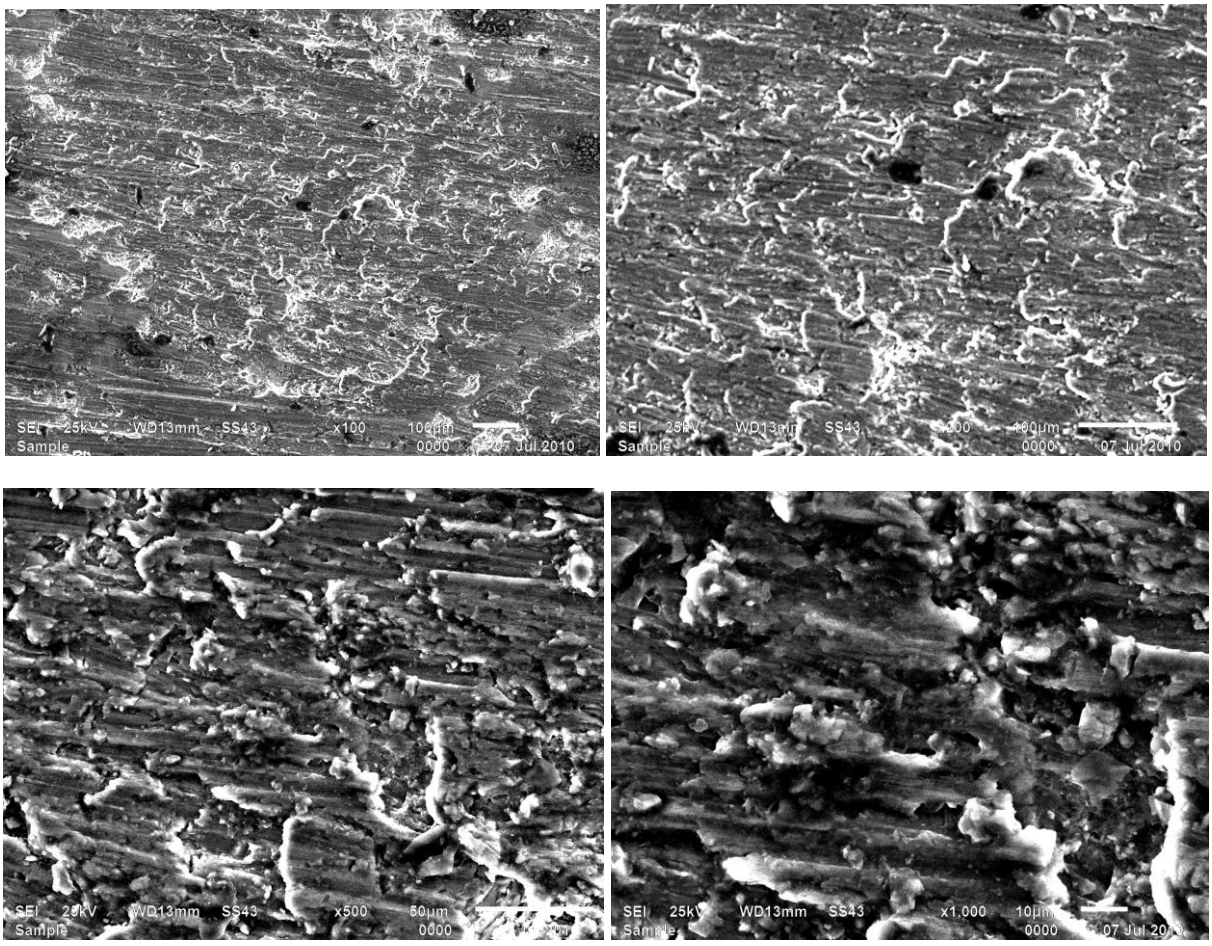

Figur 5.30 – SEM images of Sample No. 3(Before Thermal Cycling)

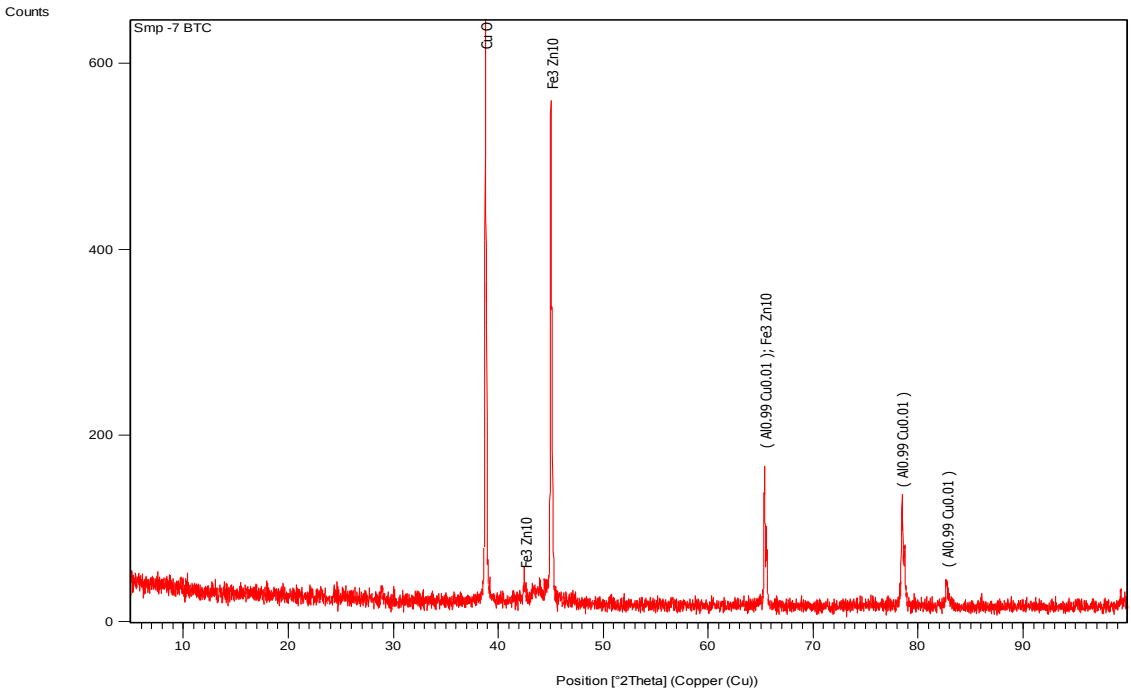

Figure 5.31- XRD graph of Sample No. 3 (Before Thermal cycling)

Table No.5.6- %age of material in Sample no. 3(Before Thermal cycling)

Visible	Ref. Code	Score	Compound Name	Displacement [°2Th.]	Scale Factor	Chemical Formula	SemiQuant [%]
*	01-080-1268	7	Copper Oxide	0.000	0.858	Cu O	74
*	01-074-5170	13	Aluminum Copper	0.000	0.285	(Al0.99 Cu0.01)	24
*	01-071-0399	36	Iron Zinc	0.000	0.035	Fe3 Zn10	2

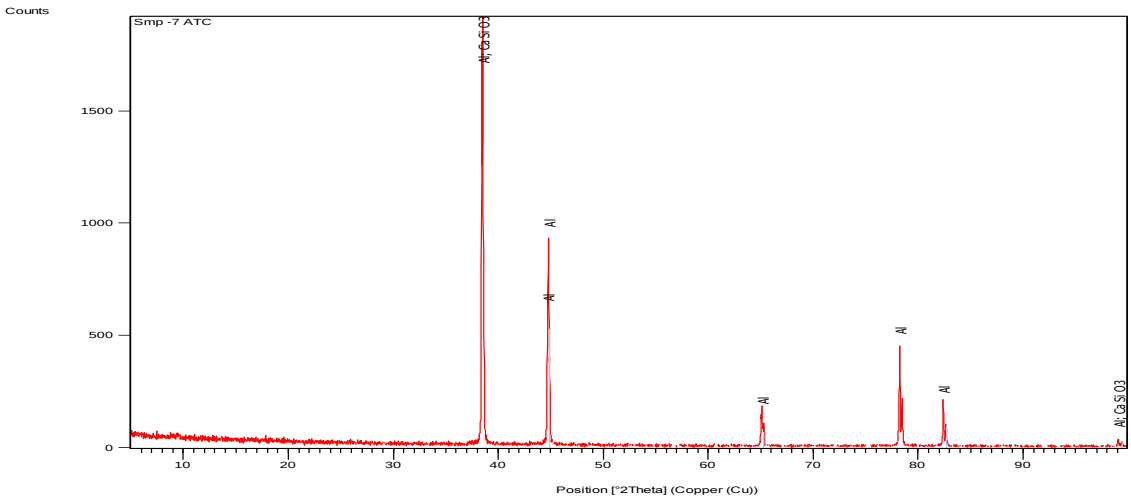

Figure-5.32- XRD graph of Sample No-3(After thermal Cycling)

Table 5.7- %age of material in Sample no. 3(After Thermal cycling)

Visible	Ref. Code	Score	Compound Name	Displacement [°2Th.]	Scale Factor	Chemical Formula	SemiQuant [%]
*	01-071-3760	84	Aluminum	0.000	0.659	Al	24
*	01-075-4975	16	Calcium Silicon Oxide	0.000	0.910	Ca Si O3	76

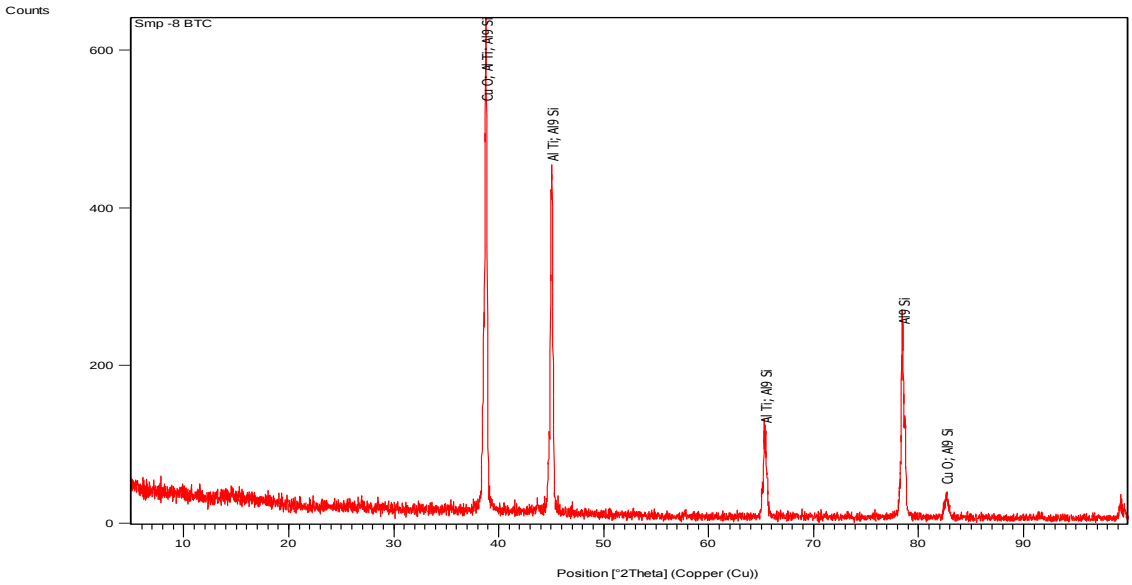

Figure 5.33-XRD garph of Sample No.4(BeforeThermal Cycling)

Table 5.8- %age of material in Sample no. 4(Before Thermal Cycling)

Visible	Ref. Code	Score	Compound Name	Displacement [°2Th.]	Scale Factor	Chemical Formula	SemiQuant [%]
*	01-089-5897	13	Copper Oxide	0.000	0.792	Cu O	47
*	01-072-5004	42	Aluminum Titanium	0.000	0.726	Al Ti	29
*	03-065-8554	85	Silicon Aluminum	0.000	0.456	Al9 Si	24

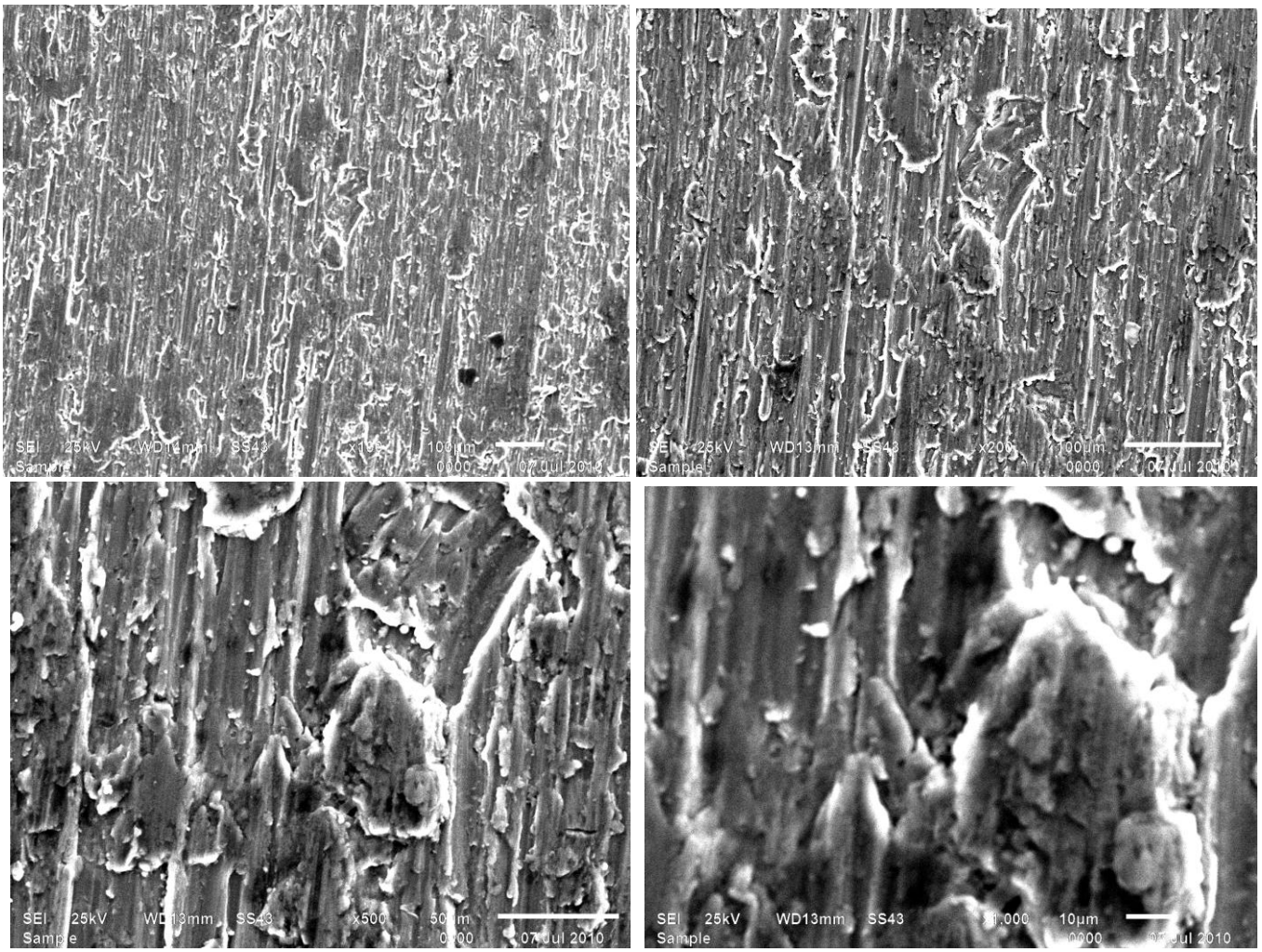

Figure 5.34-SEM images of Sample no.4(After Thermal cycling)

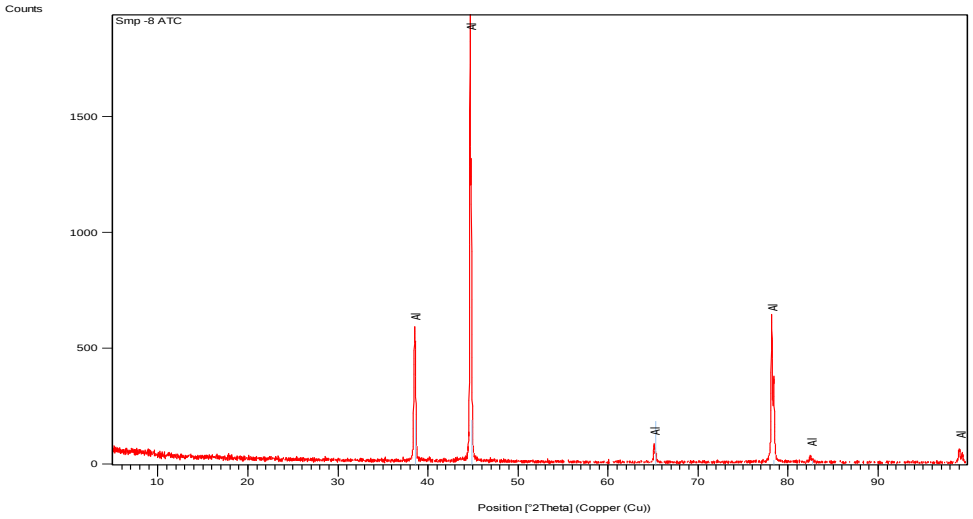

Figure- 5.35- XRD graph of Sample No. 4(After Thermal cycling)

Table 5.9- %age of material in Sample no.4 (After thermal cycling)

Visible	Ref. Code	Score	Compound Name	Displacement [°2Th.]	Scale Factor	Chemical Formula	SemiQuant [%]
*	01-071-3760	96	Aluminum	0.000	0.512	Al	100

5.3. Micro Hardness Test

The term micro hardness test usually refers to static indentations made with loads not exceeding 1 kgf. The testing is done on a microscopic scale with higher precision instruments. The surface being tested generally requires a metallographic finish and it was done with the help of 100,220P, 500, 800, 1000 & 1500 grit size emery paper. Load used on micro hardness machine used was 200 gms. Pictures of the machine on which micro hardness test was done are the following:

Figure 5.36- Pictorial view of Vicker's Microhardness Tester

The results obtained on Micohardness test are as follows:

Table-5.10- Results of Vicker's Microhardness Test.

Micro hardness	Before Thermal Cycling			After Thermal Cycling		
Sample 1 to 4	**Measure-ent 1**	**Measur-Ment 2**	**Average of Measurement - 1 and Measurement - 2**	**Measurement - 1**	**Measurment -2**	**Average of Measurement - 1 and Measurement - 2**
Aluminium=85%, SiC=15%, Fly Ash= Nil	4.388344	4.85364	4.620992	4.809204	4.566082	4.687643
Aluminium=85%,SiC =10%, Fly Ash=5%	5.42929	6.594977	6.0121335	6.556491	5.114543	5.835517
Aluminium=85%,SiC =5 %,Fly Ash =10 %	6.310755	6.555427	6.433091	4.47589	5.322582	4.899236
Aluminium=85%,SiC =Nil Fly Ash = 15 %	4.830728	5.473999	5.1523635	4.345531	4.779255	4.562393

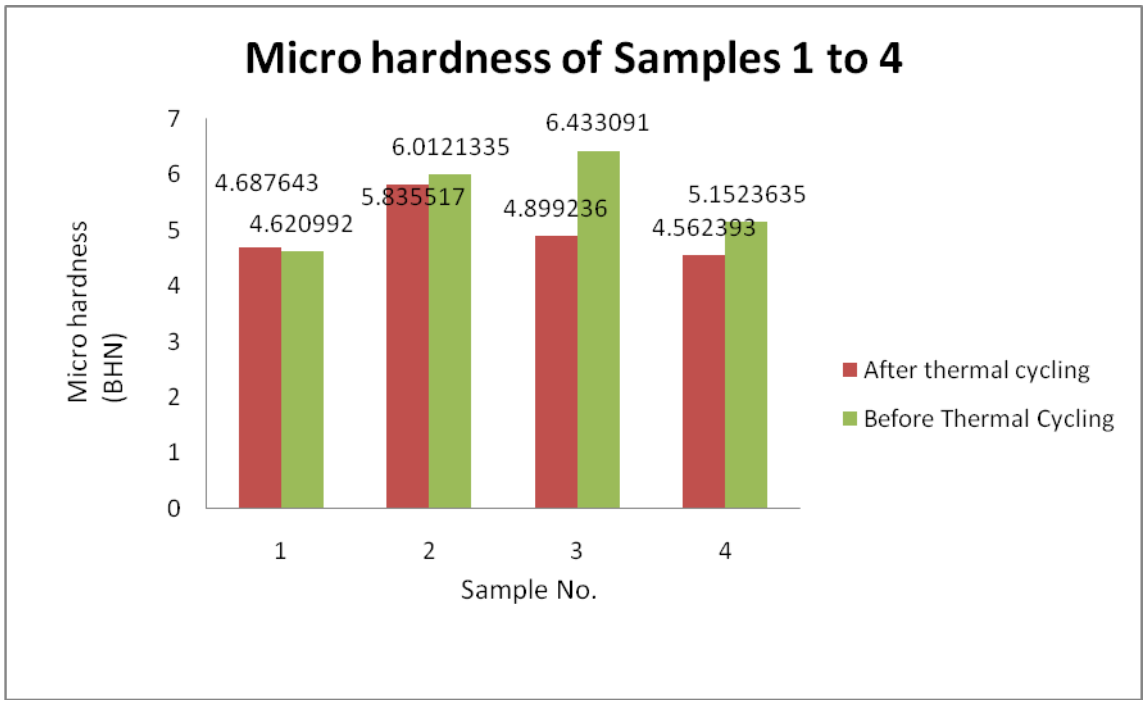

Figure 5.37 –Comparison of Microhardness of Samples 1 to 4.

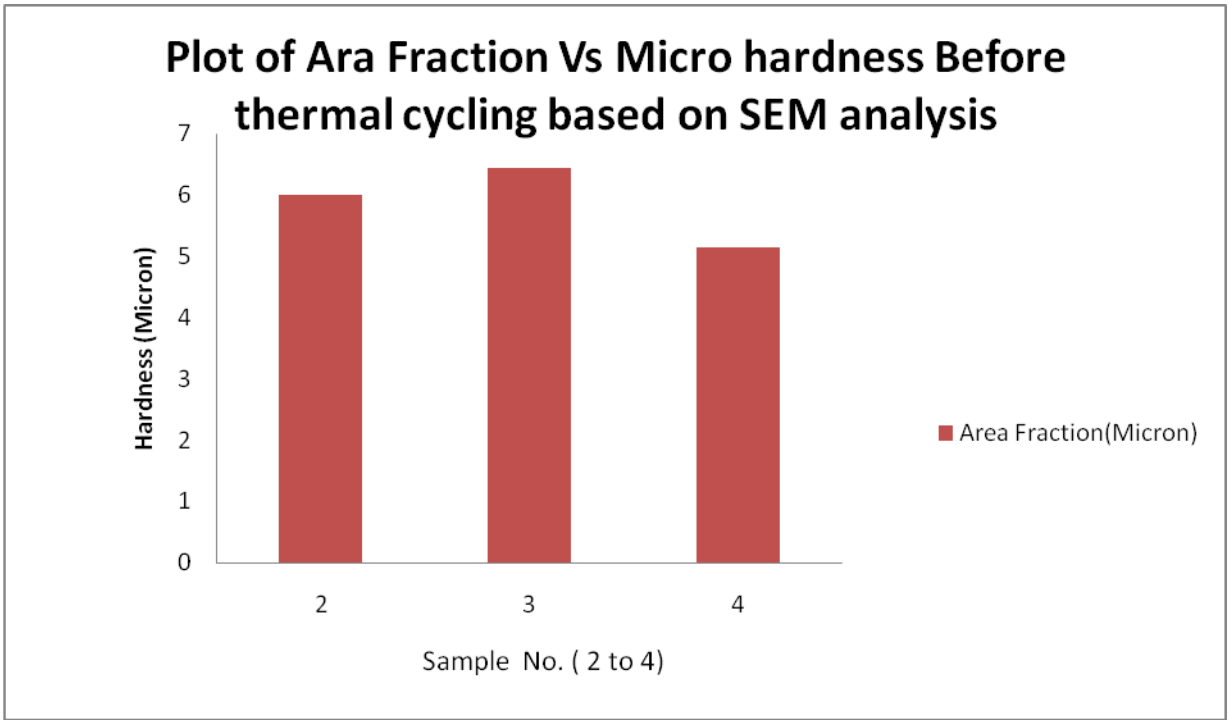

Figure 5.38 – Micro Hardness Vs area Fraction Plot of Sample no. 2 to 4 (BTC)based on SEM analysis

5.4. Wear Testing

Wear is the erosion of material from a solid surface by the action of another surface. It is related to surface interactions and more specifically the removal of material from a surface as a result of mechanical action. The need for mechanical action, in the form of contact due to relative motion, is an important distinction between mechanical wear and other processes with similar outcomes.

5.4.1 Results of Wear testing of Samples 1 to 4

Wear testing was done on the samples from 1 to 4 before and after thermal cycling. The comparative graphs of cumulative wearing of samples before thermal cycling are presented at Figure 5.14 & after thermal cycling at figure 5.15.

Table 5.11- Wear Testing of Sample no.1 Before Thermal cycling

Initial weight of Sample (gm)	**Length (mm)**	**Diameter (mm)**	**Volume (m3)**	**Speed (rpm)**	**Loading (Kg)**	**Mass of Sample (Kg)**	**Density (Kg/m3)**
9.6344	45.9	9.72	0.0034042	300	5	0.0009821	0.28849666

Time(Min)	**Weight**	**Sliding Distance**	**Weight Change**	**Wear**	**Cumulative wear**
3	9.6286	270	0.0058	0.00000149	0.00000149
6	9.5920	540	0.0424	0.00000544	0.00000693
9	9.5587	810	0.0757	0.00000648	0.00001341
12	9.5435	1080	0.0909	0.00000583	0.00001925
15	9.5402	1350	0.0942	0.00000484	0.00002408
18	9.4892	1620	0.1452	0.00000621	0.00003030
21	9.4886	1890	0.1458	0.00000535	0.00003565
24	9.4910	2160	0.1434	0.00000460	0.00004025
27	9.4879	2430	0.1465	0.00000418	0.00004443

`

Table 5.12- Wear Testing of Sample no.2 Before Thermal cycling

Initial weight of Sample (gm)	Length (mm)	Diameter (mm)	Volume (m3)	Speed (rpm)	Loading (Kg)	Mass of Sample (Kg)	Density (Kg/m3)
8.603	41.82	9.82	0.00316575	300	5	0.00087696	0.27701562

Time(Min)	Weight	Sliding Distance	Weight Change	Wear	Cumulative wear
3	8.5489	270	0.0541	0.00001447	0.00001447
6	8.4793	540	0.1237	0.00001654	0.00003101
9	4.4788	810	4.1242	0.00036760	0.00039861
12	8.4268	1080	0.1762	0.00001178	0.00041039
15	8.4132	1350	0.1898	0.00001015	0.00042054
18	8.3698	1620	0.2332	0.00001039	0.00043093
21	8.2722	1890	0.3308	0.00001264	0.00044357
24	8.1845	2160	0.4185	0.00001399	0.00045756
27	8.1168	2430	0.4862	0.00001445	0.00047200
30	8.0926	2700	0.5104	0.00001365	0.00048565

Table 5.13- Wear Testing of Sample no.3 Before Thermal cycling

Initial weight of Sample (gm)	Length (mm)	Diameter (mm)	Volume (m3)	Speed (rpm)	Loading (Kg)	Mass of Sample (Kg)	Density (Kg/m3)
9.5025	46.9	9.82	0.0035503	300	5	0.00096865	0.27283708

Time(Min)	Weight	Sliding Distance	Weight Change	Wear	Cumulative wear
3	9.3697	270	0.1328	0.00003605	0.00003605
6	9.2464	540	0.2561	0.00003477	0.00007082
9	8.9550	810	0.5475	0.00004955	0.00012037
12	8.7645	1080	0.7380	0.00005009	0.00017046
15	8.7225	1350	0.7800	0.00004235	0.00021281
18	8.5609	1620	0.9416	0.00004261	0.00025542
21	8.3630	1890	1.1395	0.00004420	0.00029961
24	8.1997	2160	1.3028	0.00004421	0.00034383
27	8.1129	2430	1.3896	0.00004192	0.00038575
30	7.9525	2700	1.5500	0.00004208	0.00042783

Table 5.14- Wear Testing of Sample no.4 Before Thermal cycling

Initial weight of Sample (gm)	Length (mm)	Diameter (mm)	Volume (m3)	Speed (rpm)	Loading (Kg)	Mass of Sample (Kg)	Density (Kg/m3)
7.8506	37.52	9.74	0.00279415	300	5	0.00080027	0.28640688

Time(Min)	Weight	Sliding Distance	Weight Change	Wear	Cumulative wear
3	7.7198	270	0.1308	0.00003383	0.00003383
6	7.7196	540	0.1310	0.00001694	0.00005077
9	7.4019	810	0.4487	0.00003868	0.00008945
12	7.2971	1080	0.5535	0.00003579	0.00012524
15	7.1742	1350	0.6764	0.00003499	0.00016023
18	7.0064	1620	0.8442	0.00003639	0.00019662
21	6.7974	1890	1.0532	0.00003891	0.00023553
24	6.4063	2160	1.4443	0.00004669	0.00028222
27	6.2460	2430	1.6046	0.00004611	0.00032834
30	6.0720	2700	1.7786	0.00004600	0.00037434
33	5.9581	2970	31.5619	0.00074208	0.00111642

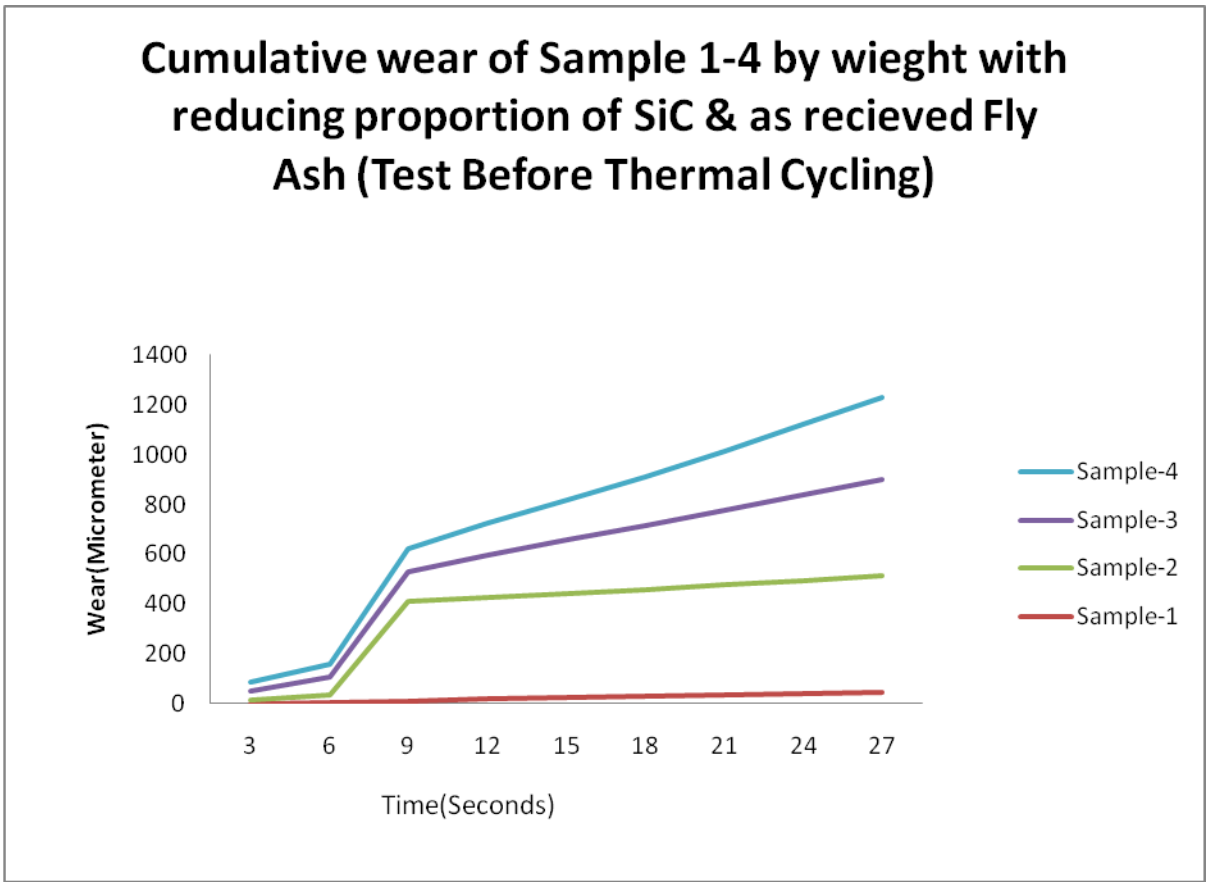

`

Figure 5.39- Comparative graph of cumulative wear w.r.t. Time

Table 5.15- Wear Testing of Sample no.1 After Thermal Cycling

Initial weight of Sample (gm)	**Length (mm)**	**Diameter (mm)**	**Volume (m3)**	**Speed (rpm)**	**Loading (Kg)**	**Mass of Sample (Kg)**	**Density (Kg/m3)**
8.7189	41.62	9.8	0.003138	300	5	0.000889	0.283249
Time(Min)	**Weight**		**Sliding Distance**	**Weight Change**	**Wear**	**Cumulative wear**	
3	8.5555		270	0.1634	0.00004273	0.00004273	
6	8.4449		540	0.2740	0.00003583	0.00007856	
9	8.2033		810	0.5156	0.00004495	0.00012351	
12	8.0636		1080	0.6553	0.00004284	0.00016635	
15	7.8807		1350	0.8382	0.00004384	0.00021019	
18	7.7348		1620	0.9841	0.00004289	0.00025308	
21	7.5964		1890	1.1225	0.00004194	0.00029502	
24	7.4898		2160	1.2291	0.00004018	0.00033520	
27	7.3707		2430	1.3482	0.00003918	0.00037437	
30	7.2035		2700	1.5154	0.00003963	0.00041400	

Table 5.16- Wear Testing of Sample no.2 After Thermal Cycling

Initial weight of Sample (gm)	**Length (mm)**	**Diameter (mm)**	**Volume (m3)**	**Speed (rpm)**	**Loading (Kg)**	**Mass of Sample (Kg)**	**Density (Kg/m3)**
9.083	43.7	9.57	0.003142	300	5	0.000926	0.294704
Time(Min)	**Weight**	**Sliding Distance**		**Weight Change**	**Wear**	**Cummulative wear**	
3	9.0365	270		0.0465	0.00001169	0.00001169	
6	8.8493	540		0.2337	0.00002937	0.00004106	
9	8.6567	810		0.4263	0.00003572	0.00007678	
12	8.5223	1080		0.5607	0.00003523	0.00011201	
15	8.3789	1350		0.7041	0.00003540	0.00014740	
18	8.2800	1620		0.8030	0.00003364	0.00018104	
21	8.1426	1890		0.9404	0.00003377	0.00021481	
24	7.9821	2160		1.1009	0.00003459	0.00024940	
27	7.8343	2430		1.2487	0.00003487	0.00028427	
30	7.7184	2700		1.3646	0.00003430	0.00031857	

`

Table 5.17- Wear Testing of Sample no.3 After Thermal Cycling

Initial weight of Sample (gm)	Length (mm)	Diameter (mm)	Volume (m3)	Speed (rpm)	Loading (Kg)	Mass of Sample (Kg)	Density (Kg/m3)
8.5073	40	9.8	0.003016	300	5	0.000867	0.287568

Time(Min)	Weight	Sliding Distance	Weight Change	Wear	Cumulative wear
3	8.4823	270	0.0250	0.00000644	0.00000644
6	8.4814	540	0.0259	0.00000334	0.00000978
9	8.4816	810	0.0257	0.00000221	0.00001198
12	8.4798	1080	0.0275	0.00000177	0.00001375
15	8.4796	1350	0.0277	0.00000143	0.00001518
18	8.4795	1620	0.0278	0.00000119	0.00001637
21	8.4753	1890	0.0320	0.00000118	0.00001755
24	8.4748	2160	0.0325	0.00000105	0.00001860
27	8.4737	2430	0.0336	0.00000096	0.00001956
30	8.4724	2700	0.0349	0.00000090	0.00002046

Table 5.18- Wear Testing of Sample no.4 After Thermal Cycling

Initial weight of Sample (gm)	Length (mm)	Diameter (mm)	Volume (m3)	Speed (rpm)	Loading (Kg)	Mass of Sample (Kg)	Density (Kg/m3)
6.418	30.98	9.68	0.002279	300	5	0.000654	0.287097

Time(Min)	Weight	Sliding Distance	Weight Change	Wear	Cumulative wear
3	6.2644	270	0.1536	0.00003963	0.00003963
6	6.1182	540	0.2998	0.00003868	0.00007831
9	5.8444	810	0.5736	0.00004933	0.00012764
12	5.7043	1080	0.7137	0.00004604	0.00017367
15	5.5128	1350	0.9052	0.00004671	0.00022038
18	5.3041	1620	1.1139	0.00004790	0.00026828
21	5.1667	1890	1.2513	0.00004612	0.00031440
24	4.8338	2160	1.5842	0.00005109	0.00036550
27	4.7609	2430	1.6571	0.00004751	0.00041300
30	4.4378	2700	1.9802	0.00005109	0.00046409

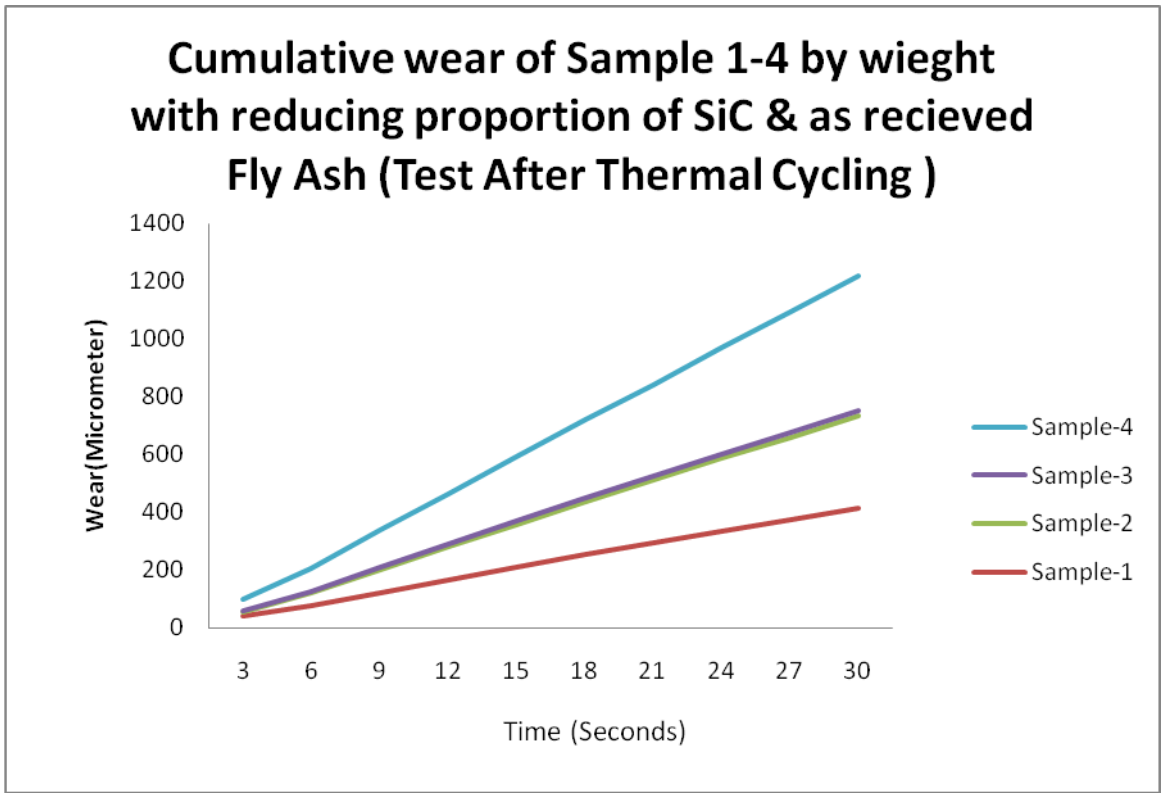

Figure 5.40- Comparative graph of cumulative wear w.r.t. Time(After Thermal Cycing)

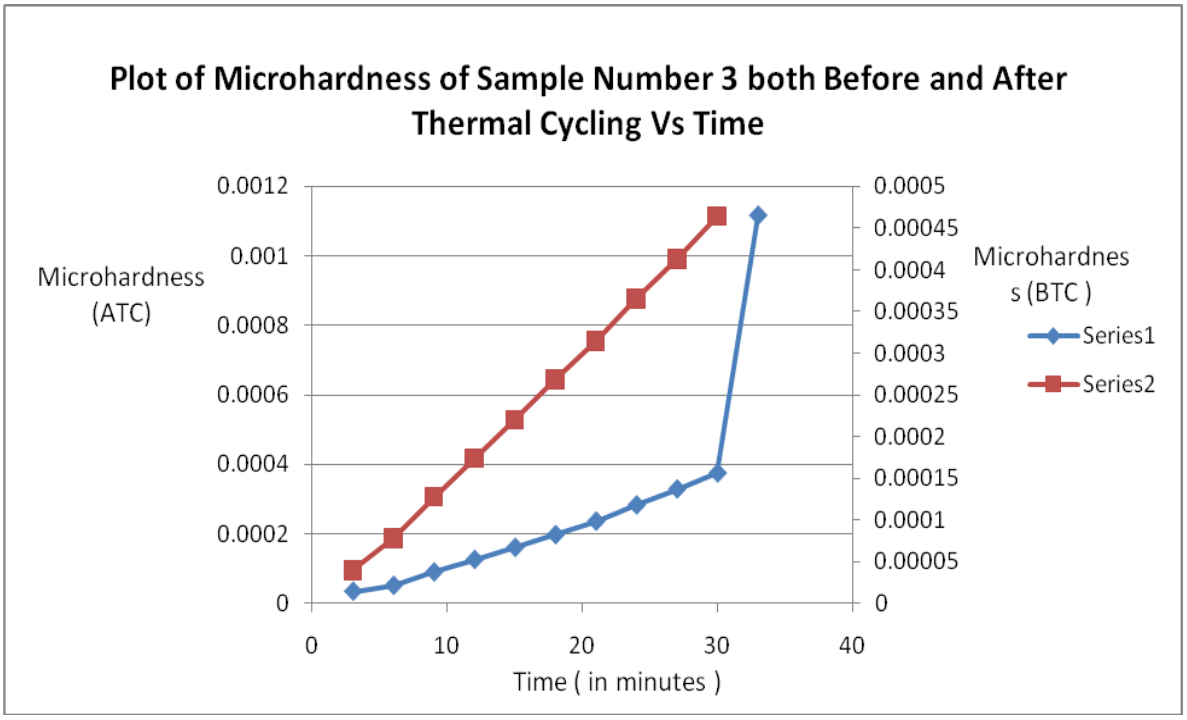

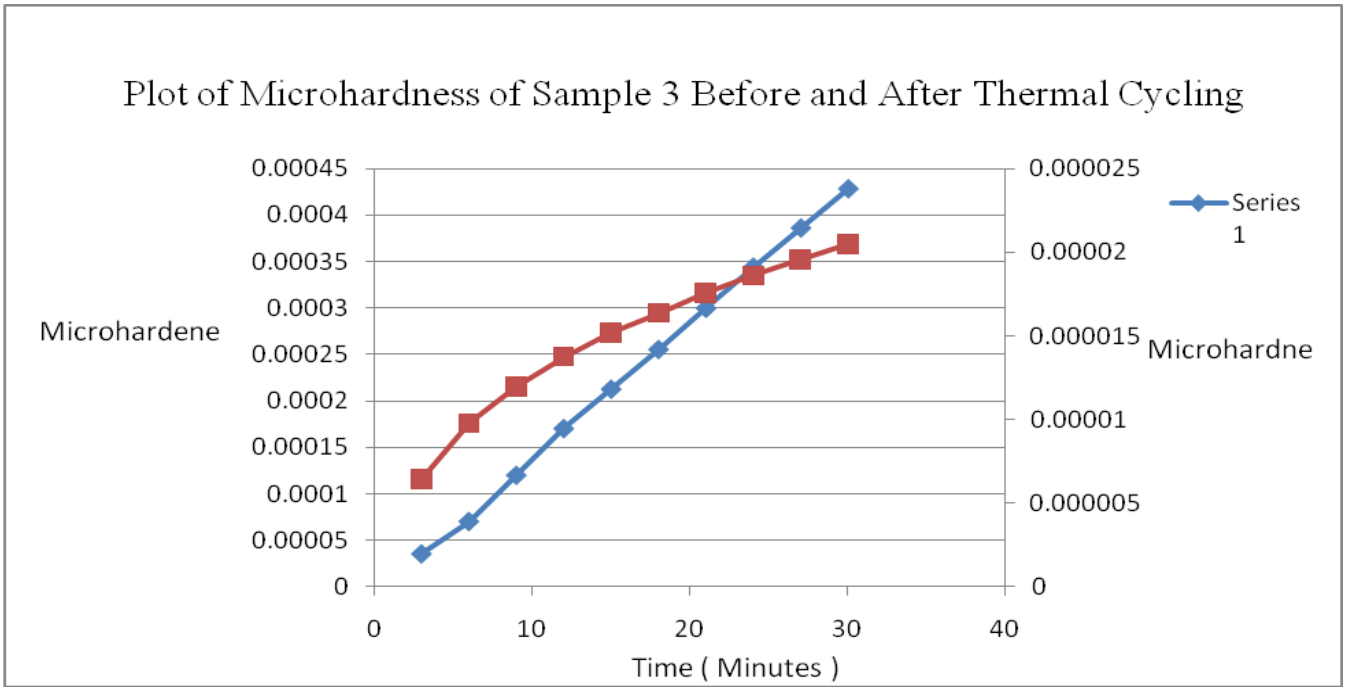

As observed from wear tests ,addition of flyash to specimen in higher percentage decreases their wear resistance.But when the spcimens were tested for after termal cycling the resistance to wear of specimen number 1 and 4 decreasd whreas of specimen number 2 & 3 increased by small amounts.Threfore ,there is need to carry out more number of expriments to genralize the effect of thermal cycling on wear resistance.

CHAPTER 6 CLOSURE

6.1 CONCLUSION:

From the experiments conducted following conclusions have been obtained:

1. The specimen with 15 % Flyash Content were found to be more stable under compressive loading and higher temperature as compared to other three specimen tested.
2. The SEM images revealed that both SiC and Fly Ash particles are well distributed in Aluminium Matrix.
3. Increase in area fraction of reinforcement in matrix result in improved harrdness values.
4. With the addition of Flyash with higher percentage the rate of heat transfer from specimens decreases as revealed by temperature time plot for heating and cooling.
5. A decrease in hardness of each specimen was found after thermal cycling. Addition of Flyash particles upto 10 % resulted in an increase in microhardness of specimens .A decrease in microhardness of every specimen was found after thermal cycling.
6. With the addition of Flyash to Al-SiC the wear resistance of the composite decreased. The specimen with highest percentage of flyash worn out more rapidly as compared to the other specimens during wear test.
7. XRD results showed negligible changes in contents of constituents before and after thermal cycling.

6.2 SCOPE OF FUTURE WORK:

1) Other Metal Matrix Composites can be manufactured and tested by using stir casting method.

2) The loading on specimens can change and the effect of thermal cycling can be observed.

`

REFERENCES

References

1. Mechanics of Composite Materials, Autar K.Kaw, CRC Press,Boca Raton,New York

2. Basics of Metal Matrix Composites, Karl Ulrich Kainer

3. [Sudip Kumar,J.Ananada Theerthan][Production and Characterization of Aluminum Fly-ash composite using stir casting method][National Institute of Engineering and Technology,Rourkela][2008]

4. [N. L. Han, Z. G. Wang, W. L. Wang, G. D. Zhang, C. X. Shi][Low-cycle fatigue behaviour of a particulate SiC/2024Al composite at ambient and elevated temperature][Composites Science and Technology][1999]

5. [Céline A.Mahieux][Environmental Degradation of Industrial Composites][Effect of temperature on polymer matrix composites][2005]

6. [Rajendra U Vaidya, K.K Chawla][Thermal expansion of metal-matrix composites][Composites Science and Technology][1994]

7. [Elhem Ghorbel][Interface degradation in metal-matrix composites under cyclic thermo-mechanical loading][Composites Science and Technology][1997]

8. [Tran Huu Nam, Guillermo Requena, Peter Degischer][Thermal expansion behaviour of aluminum matrix composites with densely packed SiC particles][Composites Part A: Applied Science and Manufacturing][2008]

9. [S. Elomari, M. D. Skibo, A. Sundarrajan, H. Richards][Thermal expansion behaviour of particulate metal-matrix composites][Composites Science and Technology][1998]

10. [Y. C. Qin, S. Y. He, D. Z. Yang][Effect of thermal–mechanical cycling on thermal expansion behaviour of boron fiber-reinforced aluminium matrix composite][Materials Chemistry and Physics][2004]

11. [S. Hertz-Clemens, C. Aumont, L. Remy][Damage mechanisms under thermal-Mechanical fatigue in a unidirectionally reinforced SiC-titanium metal matrix composite for advanced jet engine components][European Structural Integrity Society][2002]

12. [S. Q. Wu, Z. S. Wei, S. C. Tjong][The mechanical and thermal expansion behaviour of an Al–Si alloy composite reinforced with potassium titanate whisker][Composites Science and Technology][2000]

13. [H. Mykura, N. Mykura][Thermal expansion and stress relaxation of metal-matrix composites][Composites Science and Technology][1992]

14. [A.R.S. Ponter, F.A. Leckie][Bounding properties of metal-matrix composites subjected to cyclic thermal loading][Journal of the Mechanics and Physics of Solids][1998]

15. [A. R. S. Ponter, F. A. Leckie][On the behaviour of metal matrix composites subjected to cyclic thermal loading][Journal of the Mechanics and Physics of Solids][1998]

16. [N. L. Han, Z. G. Wang, G. D. Zhang][Effect of reinforcement size on the elevated-temperature tensile properties and low-cycle fatigue behaviour of particulate SiC/Al composites][Composites Science and Technology][1997]

17. [S. Jansson, D.J. Dal Bello, F.A. Leckie][Transverse and cyclic thermal loading of the fiber reinforced metal-matrix composite SCS6/Ti-15-3][Acta Metallurgica et Materialia][1994]

18. [W.A. Uju, I.N.A. Oguocha][Thermal cycling behaviour of stir cast Al–Mg alloy reinforced with fly ash][Materials Science and Engineering: A][2009]

19. [M. J. Tan, M. C. Chew, N. P. Hung, T. Sano][Thermal cycling processes in metal-matrix composites][Journal of Materials Processing Technology][1997]

20. [Y.D. Huang, N. Hort, H. Dieringa, P. Maier, K.U. Kainer][Investigations on thermal fatigue of aluminum- and magnesium-alloy based composites][International Journal of Fatigue][2006]

21. [Z. R. Xu, K. K. Chawla, A. Wolfenden, A. Neuman, G. M. Liggett, N. Chawla][Stiffness loss and density decrease due to thermal cycling in an alumina fiber/magnesium alloy composite][Materials Science and Engineering A][1995]

22. [Y. D. Huang, N. Hort, K. U. Kainer][Thermal behaviour of short fiber reinforced AlSi12CuMgNi piston alloys][Composites Part A: Applied Science and Manufacturing][2004]

23. [C. Badini, P. Fino, M. Musso, P. Dinardo][Thermal fatigue behaviour of a 2014/Al_2O_3-SiO_2 (Saffil® fibers) composite processed by squeeze casting][Materials Chemistry and Physics][2000]

24. [Pickard SM, Derby B.][The deformation of particle reinforced metal matrix composites during temperature cycling][Acta Metal Mater][1990]

25. [P. H. Shipway, A. R. Kennedy and A. J. Wilkes][Sliding wear behaviour of aluminium-based metal matrix composites produced by a novel liquid route][1998]

26. [B.N.Pramila Bai, B.S. Ramasesh and M.K. Surappa][Dry sliding wear of A356-Al-SiC_p composites][1992]

27.

28. [A. Wang and H.J. Rack][Transition wear behavior of SiC-particulate- and SiC-whisker-reinforced 7091 Al metal matrix composites][1991]

29. [S. Wilson and A. T. Alpas][Effect of temperature on the sliding wear performance of Al alloys and Al matrix composites][1996]

29. [F. M. Hosking, F. Folgar Portillz, R. Wunderlin and R. Mehrabian][Composites of aluminium alloys: fabrication and wear behaviour][Springer Netherlands][1982]